# Multiple-scattering effects in interactions of intermediate-energy antinucleons with nuclei

V. P. Zavarzina and A. V. Stepanov
*Nuclear Research Institute, Russian Academy of Sciences, Moscow*

Fiz. Elem. Chastits At. Yadra **24**, 1660–1714 (November–December 1993)

The effect of multiple scattering on the characteristics of elastic scattering and annihilation—the main processes by which intermediate-energy antinucleons interact with nuclei—is described. The conditions for the applicability of different variants of the optical model [the nonrelativistic model including the binding of the nucleon scatterers and the relativistic (Dirac) model] and the Glauber–Sitenko multiple-scattering theory are analyzed. Some of the characteristics of the elastic scattering of the lightest nuclei and antinuclei on nuclei are discussed. The dominant role of strong absorption in antinucleon interactions with nuclei at intermediate energies is demonstrated. It is shown that antinucleon annihilation events occurring in the central region of the nucleus are due to antinucleons which previously have undergone quasifree scattering on the intranuclear nucleons.

## 1. INTRODUCTION

One of the most interesting problems in modern physics is the study of the interaction between matter and antimatter. Antinucleon physics at low and intermediate energies ($E_{\bar{p}} \lesssim 1$–2 GeV) has developed rapidly in the last decade. A fairly complete review of the theoretical and experimental status of this field can be found in several reviews and conference proceedings.[1–10] The studies in this area encompass a broad spectrum of physics problems, from the use of antiprotons in research in solid-state and nuclear physics to the study of esoteric problems in gravitational theory, astrophysics, and elementary-particle physics. Here we shall focus on a topic which is relatively narrow, but essential for the interpretation of results of nuclear-physics experiments: multiple-scattering effects in interactions of antinucleons with nuclear matter. Multiple scattering has already been studied a great deal in connection with the research on interactions of nucleons with nuclei which has now been going on for many years. The main result of multiple-scattering theory is the construction of an optical potential (OP), which allows the initial multiparticle problem to be reduced to a single-particle one. In the version of multiple-scattering theory developed by K. Watson *et al.* (see Ref. 11; another, more widely used version of multiple-scattering theory is discussed in Ref. 12), the following multiple-scattering series is written down for the OP:

$$V_{\text{op}} = \sum_{\alpha=1}^{A} \langle ,0|t_\alpha|0,\rangle + \sum_{\alpha\neq\beta=1}^{A} \left\langle ,0\left|t_\alpha \frac{1-P_0}{d} t_\beta\right|0,\right\rangle + \ldots \tag{1.1}$$

[$(1-P_0)/d$ is the propagator of the hadron–nucleus system in the intermediate state]. This expansion of the OP in the number of collisions of the incident hadron with the nucleons of the target nucleus enters into the single-particle Schrödinger equation for the wave function describing the elastic scattering of a hadron on a composite system: the nucleus. The summation in (1.1) runs over the nucleons of the target nucleus, which before the interaction are in the ground state $|0\rangle$, and $P_0$ is a projection operator which separates the state $|0\rangle$ from the full spectrum of target-nucleus states. Each collision with one of the $A$ nucleons of the nucleus is described by a scattering matrix $t$ which includes the binding of the nucleon scatterer in the nuclear matter. This $t$ matrix is a complicated multiparticle operator, which in some cases can be accurately approximated by $t^f$, the free hadron–nucleon scattering matrix, which is directly related to the free-particle scattering amplitude (see, for example, Ref. 13). The expansion (1.1) in these cases can be truncated at the first term

$$V_{\text{op}}^{(1)} = \sum_{\alpha=1}^{A} \langle ,0|t_\alpha^f|0,\rangle. \tag{1.2}$$

In this approximation the OP $V_{\text{op}}^{(1)}$ is referred to as the first-order optical potential in the impulse approximation.

Among the many antinucleon–nucleus interaction processes in which multiple-scattering effects appear, the most important are elastic scattering and annihilation. The second section of this review is devoted to the analysis of the results of theoretical and experimental studies of the elastic scattering of low- and intermediate-energy antiprotons on nuclei. We consider versions of phenomenological OPs (Sec. 2.1) and microscopic OPs obtained in the Dirac (relativistic) approach (Sec. 2.4) and in the nonrelativistic theory including the effect of the nuclear medium on $\bar{N}N$ scattering (Sec. 2.5). The question of the role played by the Pauli principle and nucleon–nucleon correlations is considered separately (Sec. 2.6). One subsection (Sec. 2.2) is devoted to the use of the Glauber–Sitenko multiple-scattering theory (GST; Refs. 14–16) for describing the elastic scattering of low- and intermediate-energy antinucleons by nuclei. Special attention is paid to some problems in the interaction of the lightest antinuclei with nuclei (Sec. 2.3). The first sufficiently complete experimental program to study antimatter was realized at the 70-GeV proton accelerator at ITEP in the late 1960s and early 1970s (see Ref. 17 and the literature cited therein). There, in particular, by comparing the experimental total cross sec-

 1063-7796/93/060705-24$10.00  

tions $\sigma_t(\bar{d}p)$ and $\sigma_t(\bar{p}d)$, known with high accuracy, the *CPT* theorem was checked. The antitritium and antihelium-3 nuclei were discovered, and the exponential law governing the decrease of the cross section for antinucleus production with increasing mass was established. The cross sections were measured at incident antiparticle energies $E_{\bar{p}(\bar{d})} \gtrsim 10$ GeV. The logic of the development of the program to study antimatter is dictated by the push not only to high energies, but also to intermediate and low (and ultralow) energies (Refs. 1, 18, and 19). The possibility of storing the antinuclei $^2\bar{H}$, $^3\bar{H}$, and $^3\overline{He}$ was first discussed in Ref. 20. The development of accelerator technology and progress in secondary-particle detection[20–22] lead us to hope that in the near future experiments will also be carried out in "beams" of $^3\bar{H}$ and $^3\overline{He}$ antinuclei of the same intensity as the $\bar{d}$ "beams" used for the pioneering experiments in the late 60s and early 70s (Ref. 17). The current status of the technique of moderation of beams of high-energy particles has already made it possible to perform several experiments using beams of low- and intermediate-energy antiprotons[1–10] and makes it likely that beams of thermal and superthermal antiprotons can be used for research not only in elementary-particle physics, but also in atomic and solid-state physics.[21] These suggestions, like the experiments using "beams" of high-energy antideuterons and the discoveries of the antitritium and antihelium-3 nuclei[17] have posed the problem of the theoretical study of the nature of the interaction of intermediate- and low-energy antinuclei with matter. The results of calculations in the eikonal approximation of cross sections for reactions between intermediate- and high-energy antideuterons and nuclei from $^2$H to $^{208}$Pb are given in Ref. 23. An intranuclear cascade-model analysis of the secondary-particle multiplicity distributions measured in experiments using antideuteron "beams" with momentum 12.2 GeV/$c$ and comparison with the data on hadron–nucleus interactions indicate the possible existence of a new, noncascade, antinucleon interaction mechanism inside the nucleus.[24] The results of studying the initial stage of the interaction of the lightest nuclei and antinuclei with nuclei using the optical model are given in Sec. 2.3. The total cross sections, the reaction cross sections, and the real parts of the elastic scattering amplitude at zero angle are calculated, and a comparative analysis of these parameters is carried out for nucleus–nucleus and antinucleus–nucleus interactions.[25,26]

At low and intermediate energies, interactions of antinucleons with nuclei are dominated by annihilation (Refs. 1–4 and 27), which is a consequence of the fact that the annihilation cross section $\sigma_a^{\bar{N}N}$ makes up a sizable fraction of the total antinucleon–nucleon interaction cross section $\sigma_t^{\bar{N}N}$: $\sigma_a^{\bar{N}N}/\sigma_t^{\bar{N}N} \gtrsim 0.5$ (Refs. 1 and 4). But this is not the only reason for the intensive experimental and theoretical study of antiproton annihilation on protons and nuclei. Attempts to construct quark models of $\bar{p}p$ annihilation (see, for example, the review of Ref. 1), study of the effect of nucleon–nucleon correlations on the annihilation of antiprotons (Refs. 1, 4, and 28) and the lightest antinuclei (Refs. 24, 26, and 29) on nuclei, the possible discovery of glueballs,[30] and searches for signs of the production of a drop of quark–gluon plasma inside the nucleus[1,3] are only some of the physics problems whose solution is related to progress in studying antinucleon annihilation. An adequate approach to the problems listed above requires information about the size of the contributions of "ordinary" mechanisms for antinucleon interactions with intranuclear nucleons, for example, antinucleon rescattering. Analysis of the data on the secondary charged-particle multiplicities[3,31] indicates that for the Ne nucleus, from 80% (at an antiproton energy of 180 MeV) to 87% (20 MeV) of $\bar{p}$ annihilations occur at the surface, while the remaining 20% (13%) occur inside the target nucleus. Owing to strong damping of the incident wave, most of the annihilation events inside the nucleus occur after preliminary quasifree scattering of the antiproton on an intranuclear nucleon. As a rule, processes of this type are analyzed by the intranuclear-cascade method. However, during the initial stages of the $\bar{p}$–nucleus interaction quantum mechanical effects are important, and these cannot be studied directly using classical transport theory. The results of the classical calculation must be improved, because the fraction of "anomalous" annihilation events is comparable to the fraction of annihilations inside the nucleus given above (Refs. 3, 28, and 31). In addition, the conditions for quark–gluon plasma formation as a result of processes of this type differ from those occurring in the case of annihilation near the nuclear surface. In Sec. 3.1 we present the results of the calculation of the various contributions to the cross section for annihilation of intermediate-energy antiprotons on nuclei occurring as a result of annihilation in the entrance channel after a single quasifree antinucleon scattering, and the total annihilation cross section obtained from the optical model with coupled channels.[32,33]

The striving to isolate the contributions of the simplest processes from the total reaction cross section, represented as the sum of terms of an infinite sequence of interactions of the initial particle with nucleons of the target nucleus, has stimulated the construction of a different type of statistical approach to the description of nuclear reactions (see, for example, Refs. 34–36). In Sec. 3.1 we apply such an approach[35,36] to the analysis of antinucleon annihilation processes in nuclei using the optical model. The interaction of the incident antinucleon with intranuclear nucleons before the actual annihilation event, i.e., the "initial-state interaction," is described. The study of the interaction of mesons created in the annihilation process is of great interest from both the experimental and the theoretical points of view. Section 3.2 is devoted to this question. Some auxiliary calculations are presented in the Appendix. Our conclusions are given in the final section.

## 2. ELASTIC SCATTERING OF ANTINUCLEONS ON NUCLEI

### 2.1. The phenomenological optical potential

We shall begin our discussion of the optical potential (OP) describing the elastic scattering of low- and intermediate-energy antinucleons on nuclei with the study

TABLE I. OP parameters obtained from the "best fit" of the calculated results to the experimental angular distributions for elastic scattering (Ref. 40). The values of the parameters obtained for a different fit (Ref. 37) are given in parentheses.

| Nucleus | Antiproton momentum, MeV/$c$ | MeV | MeV | $r_R$, F | $r_I$, F | $a_R$, F | $a_I$, F |
|---|---|---|---|---|---|---|---|
| $^{12}$C | 300 | 18 (25) | 109 (61) | 1,36 (1,17) | 1,10 (1,20) | 0,59 (0,61) | 0,50 (0,51) |
| $^{40}$Ca | 300 | 40 | 100 | 1,10 | 1,10 | 0,60 | 0,60 |
| $^{208}$Pb | 300 | 20 | 140 | 1,10 | 1,10 | 0,65 | 0,65 |
| $^{12}$C | 600 | 20 | 113 | 1,35 | 1,10 | 0,44 | 0,50 |
| $^{40}$Ca | 600 | 16 | 123 | 1,34 | 1,10 | 0,50 | 0,60 |
| $^{208}$Pb | 600 | 14 | 272 | 1,34 | 1,05 | 0,47 | 0,65 |

of phenomenological models of the OP. As noted in the preceding section, owing to strong absorption of $\bar{p}$ in nuclei, the experimental data on the angular distributions of antiprotons elastically scattered on nuclei allow the form of the OP to be determined only at the periphery of the nucleus. It has been found[37,38] that the data are described equally well using widely differing forms of the spatial dependence of the OP. However, in spite of their different behavior inside the nucleus, all the models of the OPs used are close to each other in the region located a distance of (2–3)$a$ from the half-density radius $R_{1/2}$, where $a$ is the diffusivity parameter. This distance corresponds to the well known strong-absorption radius.[39] All the OPs studied contain a large imaginary part Im $V_{op}$ describing the strong absorption of the antiproton wave in the nucleus and leading to large values of the reaction cross section $\sigma_R$. Since it has been found that in order to describe the data the condition $|\text{Im } V_{op}| \geqslant 2|\text{Re } V_{op}|$ must also be satisfied, all OP models with a large attractive real part must be rejected. The hopes of a possible increase of the cross section at large scattering angles and observation of effects of antiproton "orbiting" around the target nucleus also have not been confirmed.

For phenomenological analyses it is usual to parametrize the nuclear OP in the Woods–Saxon form (the inclusion of the Coulomb interaction does not lead to any fundamental difficulties, and as a rule we shall not discuss it):

$$V_{op}(r) = V_R f_R(r) + iV_I f_I(r), \qquad (2.1)$$

$$f_x(r) = (1+\exp[(r-r_x A^{1/3})/a_x])^{-1}, \quad x=R,I. \qquad (2.2)$$

Here $V_R \equiv \text{Re } V_0$, $V_I \equiv \text{Im } V_0$, and $V_0$ is the parameter describing the depth of the OP. The results of such an analysis (the "best fit" parameters) are given in Table I (Ref. 40). Of the six OP parameters ($V_R$, $r_R$, $a_R$, $V_I$, $r_I$, and $a_I$), it is sufficient to determine reliably only three, two pertaining to the imaginary part of the OP and one to the real part. The problem of nonuniqueness of the OP parameters for low- and intermediate-energy antiprotons is discussed in Refs. 41 and 42. In Table II for several nuclei we give the radius $R_t$ near which the uncertainties in the parameters of the phenomenological OPs are minimal.[40] There we also give the corresponding values of $V_R(R_t)$ and $V_I(R_t)$. The use of potentials proportional to the nuclear charge density distribution leaves great freedom in the choice of the depth parameter Re$V_0$: 30 MeV$\leqslant$Re $V_0\leqslant$70 MeV (Ref. 38). It is possible to decrease the uncertainties in the OP parameters by using the coupled-channel method to analyze jointly the data on elastic and inelastic scattering with excitation of low-lying states of the target nucleus.[37] The results of such an analysis are given in parentheses in Table I. The possibility of decreasing the uncertainty in the parameters of antiproton OPs by analyzing not only the elastic scattering data but also the data on inelastic scattering with excitation of collective states is discussed and explained in Ref. 43. The point is that the transition density for collective states, for example, in the

TABLE II. Values of the radius $R_t$ (F) and the corresponding values of $V_R(R_t)$ and $V_I(R_t)$ (MeV); reaction cross sections $\sigma_R$ (mb) (Ref. 40). The values of these parameters from Ref. 38 are given in parentheses.

| Nucleus | Antiproton momentum, MeV/$c$ | $R_t$ | $-V_R(R_t)$ | $V_I(R_t)$ | $\sigma_R$ |
|---|---|---|---|---|---|
| $^{12}$C | 300 | 3,7 (3,7) | 5±2 (3,5) | 8±1 (8,5) | 610±40 (600) |
| $^{40}$Ca | 300 | 5,0 | 4±2 | 11±1 | 1210±100 |
| $^{208}$Pb | 300 | 8,0 | 2±2 | 14±1 | 3320±200 |
| $^{12}$C | 600 | 3,5 (3,3) | 6±2 (7,8) | 15±1 (19,6) | 480±20 (500) |
| $^{40}$Ca | 600 | 5,0 (4,94) | 5±2 (6,2) | 14±1 (13,3) | 1020±50 (990) |
| $^{208}$Pb | 600 | 8,0 (8,15) | 6±2 (5,4) | 16±1 (10,2) | 2700±100 (2670) |

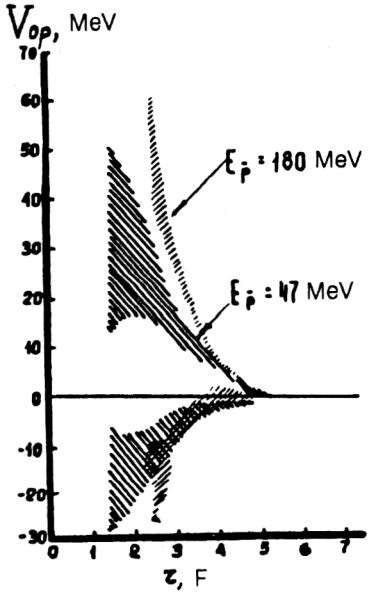


FIG. 1. OP for $\bar{p}^{12}$C at 47 MeV and 180 MeV, obtained from the Fourier–Bessel analysis. The regions where the OP is sufficiently reliably determined (Ref. 45) are shaded; Im $V_0$ is in the upper part of the figure, and Re $V_0$ is in the lower part.

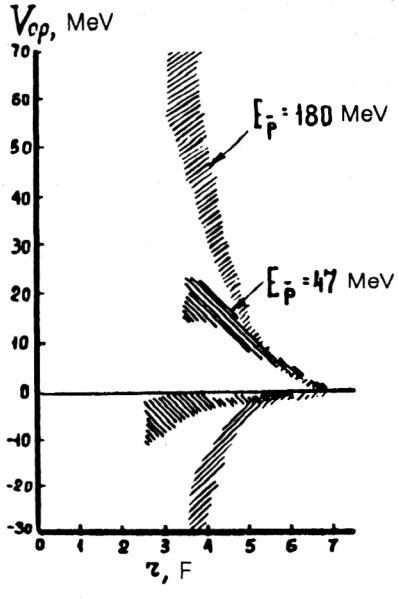


FIG. 2. The same as in Fig. 1 but for $\bar{p}^{40}$Ca.

Tassie model, is proportional to the derivative of the potential with respect to the radial variable and, accordingly, has a sharp maximum at the nuclear surface. This makes it possible to determine the "slope parameter" of the OP in the surface layer of the nucleus.

Since the presently available experimental data allow the antiproton OP to be determined reliably enough in only a relatively small region of space outside the geometrical limits of the nucleus ($r > R_{1/2}$), it is interesting the analyze the data using OPs without any restrictions on their spatial dependence. This approach includes representation of the OP as a series in some complete set of functions of the spatial coordinates. A convenient method for practical calculations is expansion in a Fourier–Bessel series:[44,45]

$$V_{\text{op}}(r) = \sum_{n=1}^{N} a_n j_0\left(n\frac{\pi r}{R_c}\right) \tag{2.3}$$

for $r \leqslant R_c$ and $V_{\text{op}}(r) = 0$ for $r > R_c$. The radius $R_c$ is taken to be sufficiently large compared with the nuclear radius, and $j_0(x)$ are the spherical Bessel functions. The complex coefficients $a_n$ have been varied using the standard $\chi^2$ minimization procedure. The number of coefficients which can be determined from the data sufficiently reliably is not large: as a rule, no more than three complex coefficients. In Figs. 1 and 2 we show the results of this analysis in the region of $r$ where the OP can be determined sufficiently reliably.

Some help in constructing a microscopic description of antiproton elastic scattering can be obtained using the folding model, where the phenomenological OP is written as a convolution integral of the charge density distribution $\rho(\mathbf{r})$, known from the results of electron scattering on nuclei, and the $t$ matrix of antiproton scattering on a nucleon bound in the nucleus:

$$V_{\text{op}} = -V_0 \int \exp(-(\mathbf{r}-\mathbf{r}')^2/s^2)\rho(\mathbf{r}')d\mathbf{r}'. \tag{2.4}$$

The Gaussian function in the integrand reflects the commonly used parametrization of the dependence of the antinucleon–nucleon scattering amplitude on momentum transfer $\hbar q$:

$$M(q) = \frac{k\sigma_t}{4\pi}(i+\alpha)\exp(-\beta q^2/2). \tag{2.5}$$

Here $\sigma_t$ is the total cross section for the scattering of antinucleons with momentum $\hbar k$, and $\alpha = \text{Re}\, M(0)/\text{Im}\, M(0)$; $\beta$ is the slope parameter of the amplitude $M(q)$. Equation (2.4) follows directly from Eq. (1.2) for the first-order optical potential. In the folding model the parameters $V_0$ and $s$ characterizing the $t$ matrix of antinucleon scattering on a nucleon bound in the nucleus are determined by fitting the calculated results to the experimental data. The results of such an analysis for $\bar{p}^{40}$Ca scattering at kinetic energy $E = 180$ MeV are given in Table III of Ref. 45. In particular, the data in that table show that the value $2\beta = 1.65$ F$^2$, corresponding to the interaction of free antinucleon and nucleon, lies between the values $s_R^2 = 2.25$ F$^2$ and $s_I^2 = 1.34$ F$^2$ obtained by comparing the calculated results with experiment. This small discrepancy might arise from differences between the neutron and proton density distributions inside the nucleus, between the $\bar{p}p$ and $\bar{p}n$ interactions, and also from the effect of the nuclear medium on the antinucleon–nucleon interaction. This effect is contained not only in the first-order OP, but also in all the higher terms of the expansion (1.1). We shall discuss this question below (in Secs. 2.5 and 2.6).

### 2.2. Description of the antiproton–nucleus interaction using the Glauber–Sitenko theory

As is well known, the applicability of the Glauber–Sitenko theory (GST) is determined by the degree to which two conditions are satisfied in a particular situation: (a) eikonality and (b) adiabaticity. The first of these conditions presupposes that the hadron trajectory in nuclear matter is a straight line, and the second corresponds to the possibility of neglecting the intranuclear motion of the nucleons of the target nucleus when the projectile passes through it. Both of these conditions are satisfied in the case of the proton–nucleus interaction with incident-particle kinetic energy $\gtrsim 1$ GeV. However, even the first applications of the GST for describing the interactions of antiprotons with deuterium,[46] $^3$He and $^3$H nuclei,[47] and especially with complex nuclei at LEAR energies (50–180 MeV; the antiproton momentum lies in the range 300–600 MeV/$c$; Refs. 2 and 48–50) turned out to be unexpectedly successful. Later the GST was used for many studies of the characteristics of various antiproton interactions with nuclei at low and intermediate energies. In the case of nuclei with $A \gg 1$, as a rule, the calculations were restricted to the so-called optical limit of the GST. In the case of elastic scattering this approximation is equivalent to the calculation of the scattering amplitude and reaction cross section using the eikonal wave functions of the optical model with first-order microscopic OP in the impulse approximation (1.2). In the case of a spherically symmetric central potential $V_c(r)$ we have the following expression for the elastic scattering amplitude $F(k,\Theta)$:

$$F(k,\Theta)=ik\int_0^\infty bdbJ_0(qb)[1-e^{i\chi_c(b)}] \tag{2.6}$$

and, accordingly, for the reaction cross section $\sigma_R$:

$$\sigma_R(k)=2\pi\int_0^\infty bdb[1-e^{-2\mathrm{Im}\chi_c(b)}], \tag{2.7}$$

where

$$\chi_c(b)=-\frac{k}{2}\int_{-\infty}^{\infty}dzU_c(b,z). \tag{2.8}$$

We have introduced the dimensionless OP

$$U_c(r)=\frac{2\varepsilon V_c(r)}{\varepsilon^2-m^2c^4}, \tag{2.9}$$

where $\varepsilon=mc^2+E_{\bar p}+E_A$, and $E_{\bar p}+E_A$ is the sum of the kinetic energies of the incident particle and the nucleus in their c.m. frame; $m$ is the mass of the incident particle. The momentum transfer $\hbar q$ is related to the incident-particle momentum $\hbar k$ by the well known expression $q=2k\sin\theta/2$. The $z$ axis is parallel to $\mathbf{k}$ ($\mathbf{k}\cdot\mathbf{b}=0$). If nonrelativistic kinematics is used to describe the scattering, instead of (2.9) we have

$$U_c(r)=\frac{V_c(r)}{E_{\bar p}}. \tag{2.10}$$

In the case of low-energy antinucleon scattering ($E_{\bar p}\lesssim 50$ MeV) the standard criterion for the eikonal approximation (EA) to be applicable, $|U|\ll 1$, $kR\gg 1$, and $kR|U|\sim 1$ (where $R$ is the nuclear radius), turns out to be violated. These constraints are softened in the case of antinucleon scattering on nuclei because of (a) the diffraction nature of the elementary $\bar NN$ scattering amplitude $M_{\bar NN}$ (Refs. 46–50) and (b) the strong absorption of antinucleons in nuclear matter.[51,52] This absorption occurs already at the nuclear surface, where the effective value of $U_c$ falls by a factor of 10–15 compared with the OP depths at the center of the nucleus.[37,38] In the standard parametrization of the amplitude

$$M_{\bar NN}(q)=\frac{k\sigma_{\bar NN}}{4\pi}(i+\alpha)e^{-\beta q^2/2} \tag{2.11}$$

the diffraction nature of $M_{\bar NN}$ is reflected in the large values of the slope parameter $\beta$, which leads to an increase of the effective value of the nuclear radius involved in the criterion for eikonality of a collision.

The applicability of the adiabatic approximation is related to a different type of cancellation of nonadiabatic and off-shell effects in the scattering amplitude (Refs. 2, 46, and 53). A detailed study of this question in the case of antinucleon scattering on complex nuclei has not yet been carried out.[2] The strong absorption in the nucleus "pushes" antinucleon–nucleon collisions to the periphery of the nucleus, where the nucleon Fermi motion is less intense owing to the low density. Therefore, in the case of interactions of antinucleons with nuclei with $A\gg 1$ it is difficult to separate the effect of the various factors which tend to soften the constraints for applicability of the GST.

To analyze the effect of the strong absorption it is useful to develop a computational technique which allows the sufficiently accurate inclusion of the contribution of the surface region of the nucleus (large values of the impact parameter $b$) to the characteristics of the antinucleon–nucleus interaction. An analytical version of this method was suggested in Refs. 51 and 52. When there is strong absorption, the profile function

$$\Gamma(b)\equiv 1-e^{i\chi_c(b)}\equiv 1-e^{-(1+i\alpha)\chi_0(b)} \tag{2.12}$$

falls rapidly from unity for $b\leqslant R$ to zero in the peripheral region of the nucleus for $b>R$. Here $\chi_0(b)=(\kappa/2)\int_{-\infty}^{\infty}dzu(\sqrt{b^2+z^2})$, where $\kappa=\rho_0\sigma_{\bar pN}$ is the absorption coefficient. This makes it possible to use integration by parts to obtain asymptotic expansions of the integrals in (2.6) and (2.7) in powers of small parameters, one of which is the ratio of the diffusivity parameter $a_0$ to the half-density radius $R_{1/2}$, and the other is the ratio of the mean free path $\kappa^{-1}$ to the length of the path traveled by the antinucleon in the diffuse layer of the nucleus, $\sqrt{\pi R_{1/2}a_0}$. The radial dependence of the function $u(r)$ in the case of nuclei with $A\gg 1$ is chosen to be of the Woods–Saxon (WS) form with effective values of the half-density radius $R_{ef}$ and diffusivity parameter $a_{ef}$:

$$u(r)=[1+\exp[(r-R_{ef})/a_{ef}]]^{-1}. \tag{2.13}$$

This trick[54] makes it possible to approximate the convolution of the Gaussian function $(2\pi\beta)^{-3/2}\exp(-r^2/2\beta)$ and the WS distribution in terms of which the function $u(r)$ is

expressed in the case of antinucleon scattering by the simple analytic expression (2.13). The values of $R_{ef}$ and $a_{ef}$ are related to $R_{1/2}$ and $a_0$, the parameters of the pointlike nucleon density distribution, as

$$R_{ef}=R_{1/2}\left(1-\frac{\beta}{R_{1/2}^2}\right), \quad a_{ef}=a_0\left[1+\frac{3}{\pi^2}\frac{\beta}{a_0^2}\right]^{1/2}. \quad (2.14)$$

Here the exact function $u(r)$ specified by the convolution integral and the function approximated in the WS form possess identical zeroth and second moments. The error in this procedure in the range of $r$ most important for calculating the scattering characteristics is 10–15%. It follows from (2.14) that $R_{ef}/R_{1/2}<1$ and $a_{ef}/a_0>1$. In the case where antiprotons with kinetic energy $E_{\bar{p}}=160$ MeV ($\beta=0.87$ F$^2$) interact with nuclei, the decrease of $R_{ef}$ relative to $R_{1/2}$ is small for heavy nuclei ($\sim 2\%$) and no more than 15% for light nuclei, and $a_{ef}$ is increased significantly: by $\sim 30\%$ for heavy nuclei and $\sim 50\%$ for light nuclei. We note that in the WS model with $\beta\neq 0$ the effective values of the rms radius

$$\langle r^2\rangle_{\beta\neq 0}^{1/2}=\left[\frac{3}{5}R_{ef}^2\left(1+\frac{7}{3}\left(\frac{\pi a_{ef}}{R_{ef}}\right)^2\right)\right]^{1/2} \quad (2.15)$$

are increased by 5–10% relative to $\langle r^2\rangle_{\beta=0}^{1/2}$.

In the range $b>R$ we can accurately write

$$u(r)\approx\exp\left(-\frac{r-R_{ef}}{a_{ef}}\right)-\exp\left(-\frac{2(r-R_{ef})}{a_{ef}}\right). \quad (2.16)$$

This approximation allows us to obtain analytic expressions for the scattering amplitude, the total interaction cross section, and the reaction cross section.[51,52] Let us give the expressions for the real part of the scattering amplitude at zero angle:

$$\begin{aligned}\mathrm{Re}\,F(0)=-kb_m a_{ef}\arctan\alpha\times\Big\{&1+\frac{a_{ef}}{b_m}(1/2+\gamma\\&+\ln\sqrt{1+\alpha^2})+(\kappa\sqrt{\pi b_m a_{ef}})^{-1}\\&\times(\alpha/\arctan\alpha)(1+\alpha^2)^{-1}\Big\}\end{aligned} \quad (2.17)$$

and for the reaction cross section:

$$\begin{aligned}\sigma_R=\pi b_m'^2\Big\{&\left[\left(1+\frac{a_{ef}}{b_m'}\right)\gamma\right]^2+\left(\frac{a_{ef}}{b_m'}\right)^2\left(\frac{\pi^2}{6}+\frac{3}{4}+\gamma\right)\\&-(a_{ef}/b_m')(\kappa\sqrt{\pi b_m' a_{ef}})^{-1}\Big\}.\end{aligned} \quad (2.18)$$

Here $\gamma=0.5772$ is the Euler constant and

$$b_m'=b_m+a_{ef}\left(1+\frac{a_{ef}}{2R_{ef}}\right)\ln 2. \quad (2.19)$$

The impact parameter $b_m$ determining the most important region of integration over $b$ is obtained from the transcendental equation

$$b_m=R_{ef}+a_{ef}\ln[\kappa\sqrt{\pi b_m a_{ef}/2}]. \quad (2.20)$$

Up to terms of order $(a_{ef}/R_{ef})^2$ we have

$$b_m\approx R_{ef}+a_{ef}(1+a_{ef}/2R_{ef})\ln[\kappa\sqrt{\pi R_{ef}a_{ef}/2}], \quad (2.21)$$

i.e., $b_m$ grows logarithmically with increasing absorption coefficient $\kappa$. Comparison of the values of the cross sections obtained analytically with the results of numerical integration showed that the accuracy of the analytic expressions in these cases is no worse than 1%. The analytic approach can also be extended to calculations of the scattering characteristics outside the EA. The noneikonal corrections to the total cross section $\sigma_t$ and the reaction cross section $\sigma_R$ in the case of strong absorption are small, while for $\mathrm{Re}\,F(0)$ these corrections are important in the region of the minima $\mathrm{Re}\,F_{(k,0)}^{\mathrm{EA}}$ (EA) and at large scattering angles.[51,52] In the limiting case of strong absorption $\kappa^{-1}\to 0$, $\alpha\to 0$, the angular distribution of elastic scattering obtained in Refs. 51 and 52 takes the form characteristic of a black sphere with diffuse boundary. The effective radius of this sphere $R_{\mathrm{sph}}$ is 1.3–1.5 times greater than the geometrical radius of the initial distribution of pointlike nucleons $R_{1/2}$. This growth of the effective radius is due to the large value of the elementary cross section $\sigma_{\bar{p}N}$, and also to the anisotropy of $\bar{p}N$ scattering. The role of the latter factor can be seen especially clearly in the case of the shell-type nucleon density, when[27]

$$\begin{aligned}\chi_c(b)=&\frac{A\sigma_{\bar{p}N}}{4\pi}(i+\alpha)\frac{1}{2\mathrm{B}}e^{-b^2/2\mathrm{B}}\left[1-\frac{\xi}{\mathrm{B}}\left(1-\frac{b^2}{4\mathrm{B}}\right)\right],\\ \xi=&\frac{A-4}{\sigma A}R_{1/2}^2, \quad \mathrm{B}=\frac{R_{1/2}^2}{4}(1+2\beta/R_{1/2}^2).\end{aligned} \quad (2.22)$$

The analytic approach to calculating the characteristics of antinucleon–nucleus elastic scattering described above has been generalized to the case of polarization observables in the scattering of antinucleons on nuclei with zero spin.[55] In this case the scattering amplitude $\mathscr{F}$ has two components: the central component $F$ and the antinucleon spin-dependent component $G$:

$$\mathscr{F}=F(q)+G(q)(\sigma\hat{\mathbf{n}}), \quad (2.23)$$

where $\hat{\mathbf{n}}=[\mathbf{k}\times\mathbf{k}']/|[\mathbf{k}\times\mathbf{k}']|$ is the unit vector in the direction of the normal to the scattering plane, $\hbar\mathbf{k}$ ($\hbar\mathbf{k}'$) is the momentum of the incident (scattered) antinucleon, and $\hbar\mathbf{q}=\hbar(\mathbf{k}-\mathbf{k}')$ is the momentum transferred to the nucleus.

In the EA the amplitudes $F$ and $G$ are defined as

$$F(k,\theta)=ik\int_0^\infty bdbJ_0(qb)[1-e^{i\chi_c(b)}\cos[kb\chi_s(b)]]. \quad (2.24)$$

$$G(k,\theta)=ik\int_0^\infty bdbJ_1(qb)e^{i\chi_c(b)}\sin[kb\chi_s(b)], \quad (2.25)$$

where

$$\chi_c(b)=-\frac{k}{2}\int_{-\infty}^{\infty}dzU_c(b,z) \quad (2.26)$$

and

$$\chi_s(b)=-\frac{k}{2}\int_{-\infty}^{\infty}dzU_{LS}(b,z). \quad (2.27)$$

Here $U_c$ and $U_{LS}$ are respectively the central and spin–orbit dimensionless OPs. In the model with microscopic first-order OP (the impulse approximation) or, equivalently, in the GST, using the common Gaussian parametrization of the components of the $\bar{p}N$ scattering amplitude

$$M_{\bar{p}N}(q)=A(q)+C(q)(\sigma[\mathbf{q}\hat{\mathbf{k}}])+\dots, \tag{2.28}$$

$$A(q)=\frac{k}{4\pi}\sigma_{\bar{p}N}(i+\alpha)\exp(-\beta q^2/2), \tag{2.29}$$

$$C(q)=\frac{k}{4\pi}\sigma_s(i+\alpha_s)\exp(-\beta_s q^2/2), \tag{2.30}$$

for the first-order OP we obtain the following expression:

$$V_{\text{op}}^{(1)}(r)=-\frac{k}{2E_{\bar{p}}}\sigma_{\bar{p}N}(i+\alpha)u(r)$$
$$+\frac{1}{2E_{\bar{p}}}\sigma_s(1-i\alpha_s)\frac{1}{r}\frac{d}{dr}u_s(r)(\sigma\mathbf{l}). \tag{2.31}$$

The analytic method of calculating the amplitude $F(k,\theta)$ for $C=0$ has a natural generalization to the case of the amplitudes $F$ and $G$ when the spin–orbit interaction is taken into account.[55] Substitution of the amplitudes $F$ and $G$ calculated for strong absorption into the expressions for the polarization

$$P=2\,\text{Re}(FG^*)/(|F|^2+|G|^2) \tag{2.32}$$

and the spin-flip function

$$Q=2\,\text{Im}(FG^*)/(|F|^2+|G|^2) \tag{2.33}$$

leads to typical expressions for $P$ and $Q$. It turns out that each of these polarization observables contains two components: one with smooth dependence on the momentum transfer, and the other oscillating about this smooth component as the scattering angle varies (see Figs. 3 and 4). Here the shape and amplitude of the oscillations are primarily related to the relative value of the slope parameters $\beta$ and $\beta_s$ of the components $A(q)$ and $C(q)$ of the elementary $\bar{p}N$ scattering amplitude. At the same time the smooth average polarization is close to the value obtained from the Kahler–Levintov theorem.[56] It is mainly determined by the ratio $\sigma_s/\sigma_{\bar{p}N}=\text{Im}\,C(0)/\text{Im}\,A(0)$ and is practically identical for all nuclei. Calculations of the antinucleon polarization in scattering on $^{40}$Ca at 150 MeV have also been carried out using the experimental information on $A(q)$ and including the results of the first polarization measurements in $\bar{p}^{12}$C scattering at this energy.[57] The results of the calculation demonstrated the effectiveness of the analytic approach for describing the absolute values and angular dependence of the antinucleon polarization. This conclusion follows from comparison of the results of the analytic calculation and numerical integration. Comparison of the results of calculating $P$ with the experimental data[57] has shown that the data at momentum 1100 MeV/$c$ can be described using the GST with $\sigma_s/\sigma_{\bar{p}N}=0.12$ F, $\beta_s=1.2$ F$^2$, and $\alpha_s=-0.1$. However, this analysis is not unique, owing to the experimental errors.

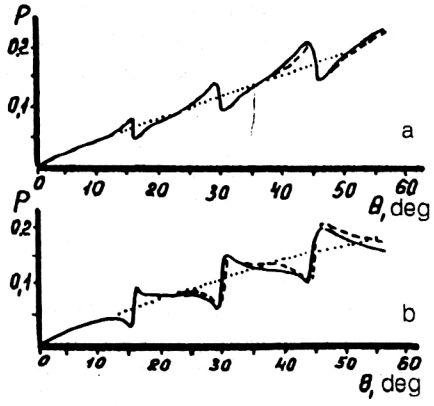


FIG. 3. Polarization in the scattering of antinucleons on $^{40}$Ca at 150 MeV, calculated for the slope parameters (a) $\beta_s<\beta$ and (b) $\beta_s>\beta$. The solid lines are the calculation using the standard GST expressions with numerical integration, the dashed lines are the calculation using the analytical expressions of Ref. 55, and the dotted lines are the average polarization $\bar{P}$ (Ref. 55).

The GST calculation of polarization observables in antiproton elastic scattering on nuclei is the subject of Refs. 58–61.

### 2.3. Collisions of the lightest nuclei and antinuclei with nuclei at intermediate energies

The total cross section $\sigma_t$, the reaction cross section $\sigma_R$, and the real part of the zero-angle scattering amplitude $\text{Re}\,F(0)$ for $^3$H($^3\bar{\text{H}}$) and $^3$He($^3\bar{\text{He}}$) collisions with nuclei at energies in the range 100–1000 MeV per nucleon have been calculated in Refs. 25 and 26. The calculations used the first-order microscopic OP of the nucleus–nucleus interaction, which is the double convolution of the densities of the interacting projectile nucleus $\rho_P(\mathbf{r})$ and the target nucleus $\rho_T(\mathbf{r})$ and the nucleon(antinucleon)–nucleon interaction matrix $t_{hN}$ (Ref. 62):

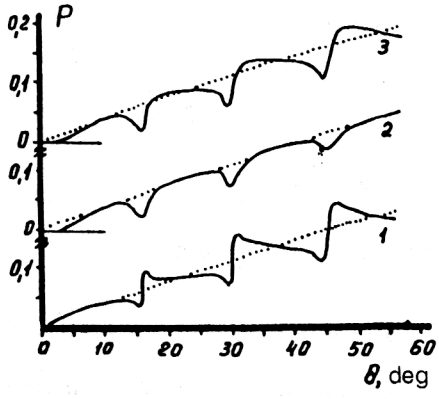


FIG. 4. Effect of the Coulomb interaction on the polarization in the scattering of antiprotons on $^{40}$Ca at 150 MeV. Curve *1* is the calculation in the GST using the analytical expressions of Ref. 55 neglecting the Coulomb interaction for $\beta<\beta_s$, and curves *2* and *3* are the calculation taking into account the Coulomb interaction respectively for $\beta=\beta_s$ and $\beta<\beta_s$; the dotted lines are the average polarization (Ref. 55).

$$V_{\rm op}(\mathbf{r}) = A_p A_T \int d\mathbf{r}_1 \int d\mathbf{r}_2 \rho_P(\mathbf{r}_1)\rho_T(\mathbf{r}_2) t_{hN}(\mathbf{r}+\mathbf{r}_1-\mathbf{r}_2). \tag{2.34}$$

The distribution of antinucleons in the antinucleus was taken to be the same as the density distribution in the corresponding nucleus. The calculations were performed both in the eikonal approximation and including the first noneikonal corrections. Let us give some of the results of these calculations (see Figs. 5–8). It follows from analysis of the curves in Fig. 5 that the energy dependence of $\sigma_R$ for nucleus–nucleus interactions mimics the behavior as a function of energy of the total cross section of the nucleon–nucleon interaction. This was pointed out in Ref. 63 and confirmed in later studies.[64–66] Analysis of the curves in Fig. 6 suggests the same conclusion regarding the reaction cross sections for interactions between antinuclei and nuclei (the results of calculations of $\sigma_R$ for interactions of $^3\bar{\rm He}$ with nuclei lead to a similar conclusion). In Figs. 7 and 8 we show the results of the calculations of Re $F(0)$ as a function of the incident-particle energy for the scattering of $^3$H and $^3\bar{\rm H}$ on $^{20}$Ne, $^{56}$Fe, and $^{208}$Pb nuclei. The principal distinguishing feature of the curves shown in these figures is the fact that the energy dependence of Re $F_{A_pA_T}$ reproduces the energy behavior of the elementary hadron–nucleon scattering amplitude averaged over neutrons and protons. The weak oscillations in Re $M_{NN}(0)$ are enhanced in the case of ion scattering (Fig. 7), and the smooth energy behavior of the function Re $M_{\bar{N}N}(0)$ is mimicked in the case of antinucleus scattering on nuclei. It is convenient to interpret these results using the analytic expression (2.17) obtained for strong absorption.[51,52] This analytic expression reproduces, with better than 3% accuracy, the results of the numerical calculation using the EA. We see that for small $\langle\alpha\rangle$, Re $F_{A_pA_T}(0) \sim \langle\alpha\rangle$ ($\langle\ldots\rangle$ denotes averaging over neutrons and protons), and both quantities simultaneously pass through zero. The fact that the energy dependence of $\langle\alpha\rangle$ is not exactly mimicked in the graphs of the function Re $F_{A_pA_T}$ is due not only to the large values of $\langle\alpha\rangle$ at certain values of the energy, but also to noneikonal effects and, mainly, to the energy dependence of the parameters $b_m$ (2.20) and the absorption coefficient $\kappa = |k\,\mathrm{Im}U(0)|$, where $U(0)$ is the dimensionless optical potential at the center of the target nucleus. It is the maximum of the mean free path $\kappa^{-1}$ in the nucleus at incident nucleon energies of 200–400 MeV which determines the enhancement of the weak oscillation in the energy dependence of Re $M_{NN}$. In the case of the elastic scattering of antinuclei on nuclei, as mentioned above, Re $F_{A_pA_T}$ depends smoothly on the incident-particle energy. We paid special attention to the analysis of the amplitude of Re $F(0)$, since it is this quantity, compared with the cross sections $\sigma_t$ and $\sigma_R$, which is particularly sensitive to the form of the spatial dependence of the OP (Refs. 27 and 67–69). The peripheral regions of the target nucleus participate in forming the real part of the zero-angle elastic scattering amplitude. In the case of antinucleus scattering these regions are farther removed from the center of the nucleus than in the case of nucleus scattering, since the densities of the target nucleus in these regions differ by several factors. Meanwhile, the mean free paths in both cases (for example, for $^3$H and $^3\bar{\rm H}$) calculated for the corresponding values of the target-nucleus density are similar. This is characteristic of strong absorption, when the important region is the periphery of the nucleus, where the density distribution can be approximated by the simple expression

$$\rho(r) \approx \rho_0[e^{-(r-R)/a} - e^{-2(r-R)/a}].$$

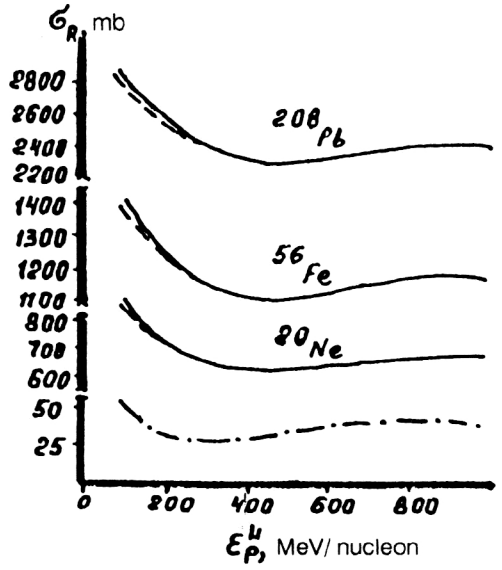


FIG. 5. Reaction cross sections for interactions of $^3$H nuclei with $^{20}$Ne, $^{56}$Fe, and $^{208}$Pb nuclei as functions of the kinetic energy of the incident nucleus per nucleon, $\varepsilon_p^L$. The solid lines are the calculation including the first noneikonal correction, and the dashed lines are the EA. The dot–dash line is the total cross section of the $pN$ interaction (Ref. 26).

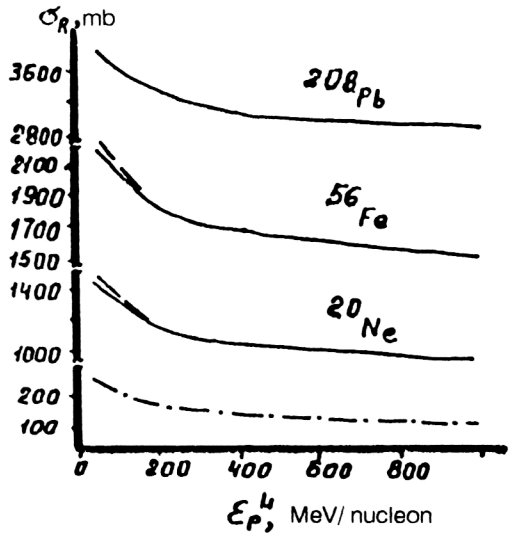


FIG. 6. The same as in Fig. 5, but for incident antinuclei $^3\bar{\rm H}$ and antiprotons (Ref. 26).

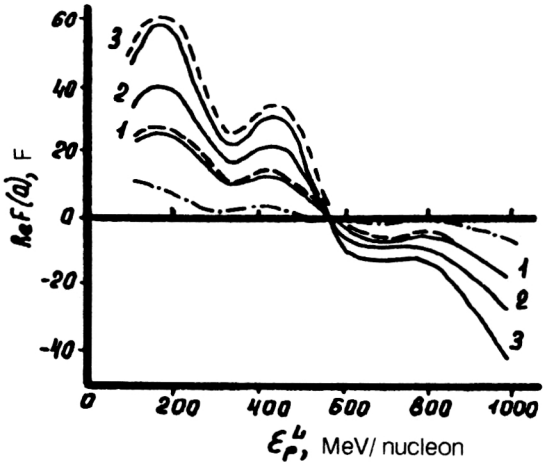


FIG. 7. Real part of the amplitude Re $F(0)$ in the c.m. frame for interactions of $^3$H nuclei with $^{20}$Ne, $^{56}$Fe, and $^{208}$Pb (curves 1–3) as a function of the energy $\varepsilon_p^L$. The solid lines are the calculation including the first noneikonal correction, and the dashed lines are the EA. The dot–dash line is the real part of the nucleon–nucleon scattering amplitude Re $M_{MN} \cdot 10$ in the $^3$H+$^{20}$Ne c.m. frame (Ref. 26).

In the region near $r \approx r_{ef} = R + a(1 + a/2R)\ln(\kappa_0\sqrt{\pi Ra/2})$, $\kappa_0 = \rho_0\sigma$ [see (2.21)], we have $(r_{ef} - R)/a \approx \ln[\kappa_0\sqrt{\pi Ra/2}]$, and $\kappa(r_{ef}) = \sigma\rho(r_{ef}) = \kappa_0[\exp[-\ln(\kappa_0\sqrt{\pi Ra/2})] - \exp[-2\ln(\kappa_0\sqrt{\pi Ra/2})]| \approx \kappa_0[1/\kappa_0\sqrt{\pi Ra/2} - (1/\kappa_0\sqrt{\pi Ra/2})^2] \approx 1/\sqrt{\pi Ra/2}$ is the value of the constant for a given nucleus, independently of the type of incident particle.

### 2.4. Relativistic models for describing the antinucleon–nucleus interaction

The successful use of relativistic methods to describe the nucleon–nucleus interaction at intermediate energies has stimulated the extension of these methods to the antinucleon–nucleus interaction. The first step in this direction was the use of the standard model of Walecka,[70] in which the motion of the incident hadron inside the nucleus is described using the Dirac equation

$$(-i\gamma^\mu\partial_\mu + M - g_\sigma\sigma + g_\omega\omega^\mu\gamma_\mu)\psi = 0, \tag{2.35}$$

where the $g$'s are constants describing the nucleon interaction with the neutral scalar field $\sigma$ ($g_\sigma$) and with the neutral vector field $\omega_\mu$ ($g_\omega$), and $M$ is the nucleon mass. In the mean-field approximation the hadron wave function satisfies the Dirac–Hartree equation

$$(-i\hbar c\gamma\nabla + \gamma_0 Mc^2 + \gamma_0 S + V - E)\psi(\mathbf{r}) = 0, \tag{2.36}$$

which involves a two-component optical potential: $S$ and $V$ are respectively the scalar and vector components of the OP (the fourth component of a Lorentz vector), and $\gamma$, $\gamma_0$ are the Dirac matrices. Each of the components is the convolution of the Yukawa form factor with the corresponding component of the nucleon density of the target nucleus.

The part of the $\bar{N}N$ interaction corresponding to one-boson exchange (OBE) can be obtained from the OBE part of $V_{NN}$ for the $NN$ interaction using the $G$-parity transformation (charge conjugation plus a 180° rotation in isospin space; see, for example, Ref. 71). Under the $G$-parity transformation the sign of the component $V$ changes and the central part of the OP in the equivalent Schrödinger equation for the large component of the Dirac spinor is significantly deeper than for the nucleon–nucleus OP. Accordingly, the spin–orbit part of the OP in the case of antinucleons is very small.[72] A more refined approach is that in which the OBE part of the $\bar{N}N$ potential is supplemented by a phenomenological annihilation potential $V^a_{\bar{N}N}$ such that the optical potential for the antinucleon–nucleon interaction has the form

$$V_{\bar{N}N} = \sum_{i=\pi,\sigma,\omega,\ldots} GV^{(i)}_{NN}G^{-1} + V^a_{\bar{N}N}. \tag{2.37}$$

The summation runs over all the types of meson included in the model. This potential makes it possible to calculate the $\bar{N}N$-scattering matrix $t_{\bar{N}N}$, and to obtain the first-order OP for describing the antinucleon–nucleus interaction using the Dirac equation.[73–75] The OP in the effective Schrödinger equation for the large component of the Dirac spinor is close in form to the standard WS potential. We note that the real part of the central OP here corresponds to repulsion for $E_{\bar{p}} = 46.8$ MeV, which is consistent with the results of the GST analysis. The same arguments as in Sec. 2.2 for the GST above can be advanced to justify the use of the impulse approximation at such low incident-particle energies. The scalar and vector components of the OP in the relativistic impulse approximation are deep:[74]

$$V_{(\bar{p}^{12}C)} = (354, -i54)\text{MeV}, \quad S = (-388, i86)\text{MeV}.$$

The results of calculations of the elastic-scattering differential cross sections, the analyzing power, and the spin-flip function of the antiproton in the relativistic and nonrelativistic approaches are similar, which can be attributed to the strong absorption and the weak spin–orbit interaction of antiprotons and nuclei. These parameters prove to

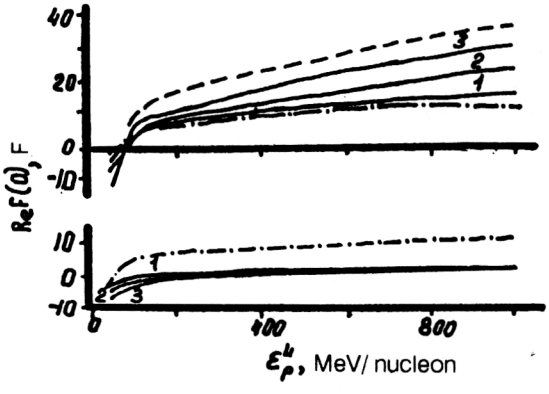


FIG. 8. The same as in Fig. 7 but for interactions of antinuclei $^3\bar{H}$ with $^{20}$Ne, $^{56}$Fe, and $^{208}$Pb (upper part). The lower part of the figure shows the real part of the amplitude Re $F(0)$ for interactions between antinucleons and nuclei. The dot–dash line is the real part of the antiproton–nucleon scattering amplitude Re $M_{\bar{N}N}(0) \cdot 10$ in the $^3\bar{H}$ + $^{20}$Ne c.m. frame (Ref. 26).

be more sensitive to the form of the model of $V_{\bar{N}N}$ (Refs. 76–81). Some of the results of these calculations[82] are given in Figs. 9–11.

We conclude by noting that the Dirac approach to describing the interaction of intermediate-energy nucleons and antinucleons with nuclei is, in spite of many successful applications, often given a negative evaluation (see Ref. 68 and the literature cited therein), mainly because of its insufficient theoretical justification. For example, in Ref. 83 it was shown that theoretically the applicability of the Dirac equation to describing the scattering of composite objects like the nucleon (or antinucleon) is very restricted and is not at all universal. In addition, in Ref. 84 it was shown that the use of even the simplest nonlocal OP in the standard nonrelativistic approach with relativistic kinematics is just as effective as the Dirac model that we have discussed.

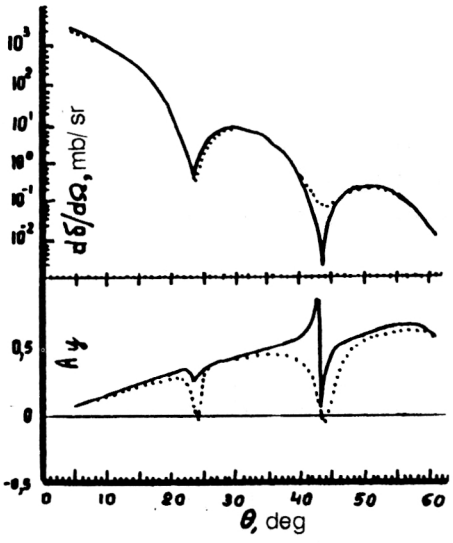


FIG. 9. Differential cross section and analyzing power of elastic $\bar{p}^{12}$C scattering at 180 MeV for first-order microscopic nonrelativistic OPs (Ref. 82). The solid line is for the Paris model of the $t$ matrix for $\bar{N}N$ scattering (Ref. 78), and the dotted line is for the Nijmegen model of the $t$ matrix for $\bar{N}N$ scattering (Ref. 79).

### 2.5. Improvement of the optical potential in the impulse approximation by inclusion of the effects of the nuclear medium

An alternative to the Dirac approach is improvement of the standard impulse approximation in multiple-scattering theory, namely, replacement of the $t$ matrix of free scattering of the incident hadron on the nucleon by the $g$ matrix describing the scattering of this hadron on a nucleon bound in the target nucleus. This idea has been developed in Refs. 85–92 for the case of low- and intermediate-energy antiproton–nucleus scattering. The nuclear medium has the greatest effect on the real part of the OP Re $V_{\text{op}}$. For example, in the impulse approximation, the OP describing the interaction of antiprotons with nucleons in the central region of the nucleus corresponds to antinucleon repulsion. At the same time the inclusion of the effects of the medium leads to an OP with antiproton attraction.

The starting point of these calculations is study of the motion of the antinucleon in nuclear matter.[85] In this case the dispersion law relating $\hbar\mathbf{k}$, the momentum of the antiproton interacting with the nuclear medium, to the antiproton energy $\bar{e}(k)$ contains the irreducible self-energy part (or mass operator) $\Sigma(\mathbf{k},\bar{e}(k),k_F)$ and has the form

$$\bar{e}(k)=\frac{\hbar^2k^2}{2M_{\bar{p}}}+\sum(\mathbf{k},\bar{e}(k),k_F). \tag{2.38}$$

Here $\hbar^2k_F^2/2M_N$ is the Fermi energy for nuclear matter. In the case of symmetric nuclear matter $k_F=[(3\pi^2/2)\rho_{NM}]^{1/3}$. For $\rho_{NM}=0.174$ nucleon/F$^3$,

$$k_F=1.371\ \text{F}^{-1}.$$

In the first approximation in the number of collisions we have

$$\sum(k,E,k_F)=\sum_{p_-<k_F}\langle\mathbf{k},\mathbf{p}_-|g(\omega)|\mathbf{k},\mathbf{p}_-\rangle. \tag{2.39}$$

Here $E$ is the antinucleon energy outside nuclear matter, $\omega=E+e(p_-)$, and $e(p_-)$ is the value of the single-particle energy of the nucleon scatterer in nuclear matter. In addition, $g(\omega)$ is the $t$ matrix of antinucleon scattering on a nucleon in nuclear matter and satisfies the equation

$$g(\omega)=V_{\bar{N}N}+V_{\bar{N}N}\sum_{p_+,p_-}\frac{Q(\mathbf{p}_-,k_F)}{\omega-\bar{e}(\mathbf{p}_+)-e(\mathbf{p}_-)+i\varepsilon}g(\omega). \tag{2.40}$$
$$\varepsilon\to 0$$

Here $V_{\bar{N}N}$ is the complex antinucleon–nucleon interaction potential (different models of this potential have been used in Refs. 76–82). The operator $Q(\mathbf{p}_-,k_F)$ takes into account the effect of the Pauli principle in intermediate states, and $\hbar\mathbf{p}_+$ and $\hbar\mathbf{p}_-$ are the antiproton and nucleon

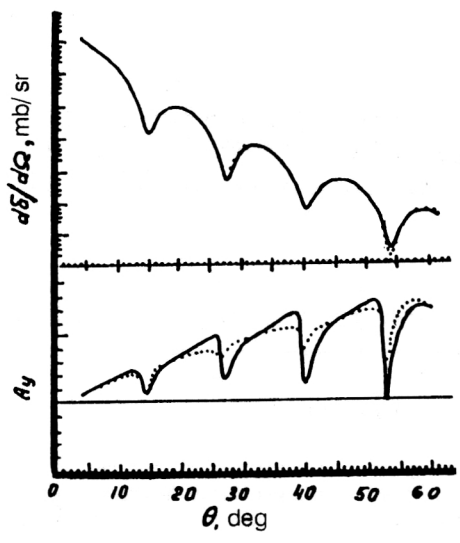


FIG. 10. The same as in Fig. 9 but for $\bar{p}^{40}$Ca.

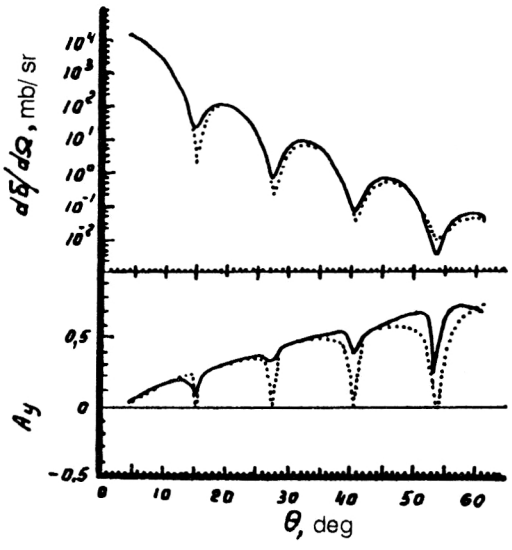


FIG. 11. Differential cross section and analyzing power of elastic $\bar{p}^{40}$Ca scattering at 180 MeV for first-order microscopic OPs (Ref. 82). The solid and dotted lines are respectively obtained for the relativistic (Dirac) model and for the nonrelativistic model.

momenta characterizing a specific intermediate state. The first-order optical potential determining the motion of the antinucleon in nuclear matter is

$$\tilde{V}_{\text{op}}(k)=\sum(k,\bar{e}(k),k_F). \tag{2.41}$$

In going from the case of nuclear matter to the description of antinucleon scattering on nuclei we use the local-density approximation, where the parameter $k_F$ is replaced by $k_F(r)=[(3\pi^2/2)\rho(r)]^{1/3}=1.371[\rho(r)/\rho(0)]^{1/3}$, where $\rho(r)$ is the target-nucleus density at the point $r$. This approach can be generalized to the case of an arbitrary single-particle model of the target nucleus.[86,87] We write the Hamiltonian $\hat{H}$ of the antinucleon–nucleus system as

$$\hat{H}=\hat{H}_0+\sum_{i=1}^{A} v_{\bar{p}i}, \tag{2.42}$$

where $\hat{H}_0=\hat{H}_{\text{nucl}}+\hat{K}_0$ is the sum of the antinucleon kinetic energy and the target-nucleus Hamiltonian $\hat{H}_{\text{nucl}}$, and $v_{\bar{p}i}$ is the potential energy of the interaction of the antinucleon with the $i$th nucleon of the nucleus. In this case the $g$ matrix satisfies the equation

$$g(\omega)=v_{\bar{p}N}+v_{\bar{p}N}G(\omega)g(\omega). \tag{2.43}$$

The Green function $G(\omega)$ is determined self-consistently using the equation

$$G(\omega)=G_0(\omega)+G_0(\omega)V_{\text{op}}G(\omega), \tag{2.44}$$

where

$$V_{\text{op}}=\langle\text{g.s.}|g(\omega)|\text{g.s.}\rangle \tag{2.45}$$

is the first-order optical potential; $|\text{g.s.}\rangle$ is the appropriately symmetrized wave function of the nuclear ground state. The Green function $G_0$ corresponds to the Hamiltonian $\hat{H}_0$. The $g$ matrix of the model can also be found from the equation

$$g=t_0+t_0G_0TG_0g, \tag{2.46}$$

where

$$T=V_{\text{op}}+V_{\text{op}}G_0T. \tag{2.47}$$

Here the $t$ matrix of $\bar{N}N$ scattering $t_0$ satisfies the Lippmann–Schwinger equation neglecting self-consistency:[87] $t_0=V_{\bar{p}N}+V_{\bar{p}N}G_0t_0$. Replacing the Green function $G$ in (2.43) by the propagator

$$G_Q=\sum_{\substack{\mathbf{p}_-\mathbf{p}_+\\ \varepsilon\to 0}}\frac{Q(\mathbf{K},\mathbf{q},k_F)}{\omega-\bar{e}(p_+)-e(p_-)+i\varepsilon}, \tag{2.48}$$

we obtain the result corresponding to nuclear matter. Here we have introduced the notation $\mathbf{q}=\frac{1}{2}(\mathbf{p}_+-\mathbf{p}_-)$, $\mathbf{K}=(\mathbf{p}_++\mathbf{p}_-)$.

In the local-density approximation the first-order optical potential is the convolution of the $g$ matrix and the target-nucleus density

$$V_{\text{op}}^{(1)}(\mathbf{r},E)=\int\{g^{\bar{p}p}(|\mathbf{r}-\mathbf{r}'|;k_F^p(r);E)\rho_p(r') +g^{\bar{p}n}(|\mathbf{r}-\mathbf{r}'|;k_F^n(r);E)\rho_n(r')\}d\mathbf{r}', \tag{2.49}$$

where we have introduced the individual densities $\rho_p(r)$ and $\rho_n(r)$ for the protons and neutrons of the target nucleus. Here we have written the OP in the local approximation, although in the general case the OP $V_{\text{op}}^{(1)}$ is a nonlocal operator. The spatial dependence of the OP is considerably different from that of the first-order OP in the impulse approximation. However, the strong absorption of antinucleons hinders their penetration into the central region of the nucleus, where this difference is more important. Near the nuclear surface, where most of the antinucleon interactions with the intranuclear nucleons occur, the effect of the medium is small, owing to the low density $\rho$ in this region.

The version of the operator $Q(\mathbf{K},\mathbf{q},k_F)$ containing averaging over angles is used for actual calculations:

$$Q(\mathbf{K},\mathbf{q},k_F)=\begin{cases}0, & |\frac{\mathbf{K}}{2}+\mathbf{q}|\leqslant k_F\\ 1, & |\frac{\mathbf{K}}{2}+\mathbf{q}|>k_F,\end{cases} \tag{2.50}$$

and, in particular,

$$Q(\mathbf{K},\mathbf{q},k_F)\to Q(K,q,k_F)$$

$$=\begin{cases} 0, & \frac{K}{2}+q\leqslant k_F \\ 1, & \left|\frac{K}{2}-q\right|>k_F \\ \frac{1}{2Kq}\left[\left(\frac{1}{2}K+q\right)^2-k_F^2\right] & \text{otherwise.} \end{cases} \tag{2.51}$$

We recall that the $\bar{p}N$ interaction is characterized by strong anisotropy of the angular dependence of the $\bar{p}N$ scattering amplitude. The effect of this anisotropy on the operator $Q$ will be discussed in the following subsection. The effects of the nuclear medium in the antinucleon–nucleus interaction do not reduce only to the effect of the Pauli principle, but also involve the nucleon scatterer in the target nucleus. In the independent-particle model it is necessary to use $e_N(p)=\hbar^2p^2/2M_N+\tilde{U}_N(p)$ in the calculations.

In the case of the scattering of low- and intermediate-energy antiprotons, the effects of the nuclear medium are very small, owing to the large contribution of annihilation to the total cross section of the $\bar{p}N$ interaction. Comparison of the results of the calculations using different forms of the $\bar{N}N$ interaction and the experimental results does not at present give us any reason to choose one particular version of the $\bar{N}N$ potential.

In conclusion, we note that the effects of the medium in the microscopic relativistic approach in the case of nucleon scattering on nuclei are taken into account by the introduction of an effective parameter (the effective mass of the scattered nucleon) in Refs. 93–95.

### 2.6. The effect of the Pauli principle and anisotropy of $\bar{p}N$ scattering on the characteristics of antiproton interactions with nuclei

As was shown in the preceding section, replacement of the $t$ matrix of free $\bar{N}N$ scattering by the $g$ matrix allows us to include corrections to the impulse approximation for the first-order microscopic OP $V_{IA}^{(1)}$ due to the effect of the nuclear medium on the $\bar{p}N$ interaction process in nuclear matter. We recall that the use of $V_{IA}^{(1)}$ in combination with the eikonal approximation for solving the wave equation of the optical model is equivalent to the optical limit of the GST. The procedure described above of finding the $g$ matrix of the interaction of an antinucleon with an intranuclear nucleon involves a significant simplification in that the anisotropy of $\bar{p}N$ scattering is neglected (see the preceding subsection). Because of the importance of this factor, it is interesting to study its effect on the size of the corrections to $V_{IA}^{(1)}$. Let us first estimate the size of the corrections to the imaginary part $\mathrm{Im}\,V_{IA}^{(1)}\equiv W_{IA}^{(1)}$, which in the nonrelativistic approximation, and assuming isotropy of the elementary $\bar{p}N$ scattering, has the form

$$W_{IA}^{(1)}(r)=\frac{2\pi}{M}\,\mathrm{Im}\,M_{\bar{p}N}(0;p)\rho(r)=\frac{p_a}{2M}\sigma_t(p)\rho(r). \tag{2.52}$$

Here $\sigma_t=\sigma_s+\sigma_a+\sigma_{\mathrm{cex}}$ is the total $\bar{p}N$-interaction cross section, $\mathbf{p}$ is the relative momentum of the colliding particles, and $p_a$ is the incident-antiproton momentum in the antiproton–nucleus c.m. frame. For simplicity here we have set $h=1$; $M$ is the nucleon mass.

Use of the standard Gaussian parametrization of the amplitude $M_{\bar{p}N}$ taking into account the anisotropy of the scattering

$$M_{\bar{p}N}(\mathbf{p}_a,\mathbf{p}_1)=M(0;p)\exp\left[-\frac{\beta}{2}(\mathbf{p}_a-\mathbf{p}_1)^2\right], \tag{2.53}$$

where $\mathbf{p}_1$ is the antiproton momentum after collision, and the procedure of Ref. 54 allowing the convolution of the Gaussian function and the WS distribution to be approximated by a new WS distribution with effective parameters $R_{ef}$ and $a_{ef}$ [see (2.14)], allows the form of (2.52) to be preserved. There are two sources of corrections to (2.52). First, corrections arise in the expression for the first-order OP owing to modification of the $\bar{p}N$-scattering amplitude in the nuclear medium. Secondly, they arise from double, triple, etc. rescatterings of the incident particle on the various nucleons of the nucleus (the contributions $V^{(2)}$, $V^{(3)}$, etc.). The simplest and most important contribution comes from inclusion of the effect of the Pauli principle on the cross section for $\bar{p}N$ scattering in the nuclear medium. The effect of the Pauli principle on the $\bar{p}N$-annihilation cross section is small, owing to the large energy release in this process, and the charge-exchange cross section $\sigma_{\mathrm{cex}}$ is small compared with $\sigma_s$ and $\sigma_a$. We shall restrict ourselves to analysis of the corrections to $W_{IA}^{(1)}$, since the real part of the microscopic OP for antiprotons is small. To obtain estimates we use the model of a homogeneous ideal Fermi gas together with the local-density approximation. We use this model to calculate $\langle\sigma_s\rangle$, the total cross section for scattering of the incident particle on a nucleon of the nucleus. This makes it possible to use (2.52) to estimate the effect of the Pauli principle on the imaginary part of the first-order OP. This program has been realized in Refs. 96–101 in the case of isotropic hadron–nucleon scattering. Taking into account (2.53), we can write

$$\begin{aligned}\langle\sigma_s\rangle=&\frac{3}{4\pi p_F^3}\frac{4}{p_a}\int d\mathbf{p}_A\int d\mathbf{p}_1\,|M_{\bar{p}N}(0,p)|^2\\ &\times\exp(-\beta(\mathbf{p}_a-\mathbf{p}_1)^2)\delta[(p_1^2-p_a^2)/2\\ &+(\mathbf{p}_1-\mathbf{p}_a)^2/2-\mathbf{p}_A(\mathbf{p}_1-\mathbf{p}_a)],\end{aligned} \tag{2.54}$$

where $p_A$ is the momentum of an intranuclear nucleon before collision and $p_F$ is the Fermi momentum.

In cases of practical interest $\beta p_a^2\gg\beta p_Fp_a\sim 1\gg\beta p_F^2$ the integration in (2.54) can be performed analytically with the result[102]

$$\begin{aligned}\langle\sigma_s\rangle=A_k\Bigg\{1-\frac{4}{5}\beta p_F^3+\mu_k\left(\frac{p_F}{p_a}\right)^2-\mathrm{e}^{-\beta p_a^2}\Bigg[\frac{3}{x^3}(x\cosh x\\ -\sinh x)+\mu_k\left(\frac{p_F}{p_a}\right)^2+(\gamma_k+\xi)\beta p_F^2\Bigg]\Bigg\}.\end{aligned} \tag{2.55}$$

We have introduced the notation $x=2\beta p_a p_F$, $\xi=1/5$ for the incident antinucleon (if a nucleon scatters on intranuclear nucleons, $\xi=1$); the subscript $k$ distinguishes different forms of the dependence $|M_k(0,p)|^2=\sigma_k(p)/4\pi$:

$$A_0=\tilde{\sigma}_0/\beta p_a^2, \quad \mu_0=0, \quad \gamma_0=-2/5, \quad \sigma_0(p)=\tilde{\sigma}_0;$$

$$A_1=(2\tilde{\sigma}_1/p_a)(1/\beta p_a^2), \quad \mu_1=1/5, \quad \gamma_1=0, \quad \sigma_1(p)=\tilde{\sigma}_1/p;$$

$$A_2=(4\tilde{\sigma}_2/p_a^2)(1/\beta p_a^2), \quad \mu_2=3/5, \quad \gamma_2=2/5,$$

$$\sigma_2(p)=\tilde{\sigma}_2/p^2.$$

The accuracy of the calculation is limited to quantities $\sim\beta p_F^2$. However, in (2.55) we have kept also the next smallest terms, because they ensure the correct passage to the limit for $\beta\to 0$ in the isotropic-scattering expressions for $p_a^2\gg p_F^2$.

The special feature of Eq. (2.55) is the preservation of the correction factor $1-\frac{4}{5}\beta p_F^2$ even for extremely high energies, which also occurs for an arbitrary form of anisotropy of $\bar{p}N$ scattering if $\beta(p_a)$ does not tend to zero. In fact, it is possible to neglect the effect of the Pauli principle when the average energy transferred in a collision $\langle\Delta E\rangle$ is large compared with the Fermi energy, which happens for $p_a^2\gg p_F^2$ in the case of isotropic scattering. In the case of anisotropic scattering (2.53) its value is $\langle\Delta E\rangle\approx 1/2\beta M$, where $M$ is the nucleon mass, and it does not grow with increasing incident-particle energy if at the same time the scattering does not become more isotropic. It follows from (2.52) and (2.55) that for values of the parameters $\beta$ and $p_a$ corresponding to the scattering of antiprotons with energy in the range 50–200 MeV, the effect of the Pauli principle on the cross section for $\bar{p}N$-scattering in the nuclear medium leads to a decrease of $W_{IA}^{(1)}$ by a factor of $[1-(4/5)\beta p_F^2(\sigma_s/\sigma_t)]^{-1}$.

The presence of correlations between the intranuclear nucleons leads in the case of isotropic scattering to the following second-order term in the OP:

$$W^{(2)}=\frac{p_a}{M}\left[\frac{2\pi}{p_a}\rho(r)M(0,p)\right]^2\int_0^\infty d\xi[g(\xi)-1]. \tag{2.56}$$

In the case of the ideal Fermi gas the integral of the correlation function $g(\xi)-1$ is equal to $-3\pi/5p_F$. The inclusion of the anisotropy in antiproton scattering on nucleons decreases Eq. (2.56) by a factor of $(1+\frac{4}{5}\beta p_F^2)$ (Ref. 103) and the correction (2.56) leads to multiplication of $W_{IA}^{(1)}$ by $1+[\sigma_t(1-\alpha^2)p_F^2/20\pi(1+\frac{4}{5}\beta p_F^2)$, where $\alpha=\mathrm{Re}M(0)/\mathrm{Im}M(0)$ (Ref. 102).

The passage to a finite nucleus in the local-density approximation requires replacement of $p_F^2$ by $p_F^2(r)=p_F^2[\rho(r)/\rho(0)]^{2/3}$. When these two corrections are combined, the imaginary part of the microscopic OP takes the form

$$W=W_{IA}^{(1)}\left\{1-\frac{4}{5}\beta p_F^2(r)\frac{\sigma_s}{\sigma_t}+\frac{\sigma_t}{20\pi}\frac{(1-\alpha^2)p_F^2(r)}{1+\frac{4}{5}\beta p_F^2(r)}\right\}. \tag{2.57}$$

At the center of the nucleus $p_F=1.371$ F$^{-1}$ and $\frac{4}{5}\beta p_F^2\approx 2$ for $E_{\bar{p}}=47$ MeV, so that Eq. (2.57) is, strictly speaking, inapplicable. It can only be stated that $W$ is decreased significantly compared with $W_{IA}^{(1)}$. In the case of strong absorption, which occurs in the scattering of low- and intermediate-energy antiprotons on nuclei, for calculating the amplitude of antiproton–nucleus scattering in the eikonal approximation it is sufficient to know the profile function only in the peripheral region of the nucleus,[51,52] where $\rho(b_m)/\rho(0)\lesssim 0.1$. The characteristic impact parameter $b_m$ is expressed in terms of the parameters of the nuclear density distribution in the WS form $R_{ef}$ and $a_{ef}$ and the total cross section of the free $\bar{p}N$ interaction (see Sec. 2.2). For large $r\sim b_m$ the two corrections to the OP in the impulse approximation (2.52) are small ($\sim$0.10–0.15) and almost completely cancel each other out, since $\sigma_s\approx\sigma_t(1+\alpha^2)/16\pi\beta$ and $\alpha^2\ll 1$. In spite of the crudeness of the approximations used in deriving (2.55)–(2.57), it is still interesting to estimate the contribution of the single term $W_{IA}^{(1)}[-(4/5)]\beta p_F^2(r)(\sigma_s/\sigma_t)$ to the antiproton–nucleus scattering amplitude. For this we use the technique of expanding in powers of the small parameters $a_{ef}/b_m$ and $[\rho(0)\sigma_t\sqrt{\pi b_m a_{ef}}]^{-1}$ (Refs. 51 and 52; see Sec. 2.2 above). The approximate expression for the relative correction to the imaginary part of the eikonal forward scattering amplitude arising from modification of the elementary $\bar{p}N$ scattering in the nuclear medium owing to the Pauli principle has the form

$$\frac{\mathrm{Im}\,\Delta F(0)}{\mathrm{Im}\,F(0)}\cong -2\frac{a_{ef}}{b_m}\frac{\sigma_s}{\sigma_t}\frac{0.88}{[\rho(0)\sigma_t\sqrt{\pi b_m a_{ef}}]^{2/3}}\frac{4}{5}\beta p_F^2. \tag{2.58}$$

An analogous expression for the relative correction to the real part of the forward scattering amplitude is obtained from (2.58) by replacing the factor $-2(a_{ef}/b_m)$ by 5/3. In the case of $\bar{p}^{40}$Ca scattering at $E_{\bar{p}}=47$ and 180 MeV we obtain the small corrections $\mathrm{Im}\,\Delta F(0)/\mathrm{Im}\,F(0)\approx -0.03$ and $\mathrm{Re}\,\Delta F(0)/\mathrm{Re}F(0)\approx 0.17$. They are independent of energy because at the same time as the slope parameter of the $\bar{p}N$ amplitude increases from 0.87 to 1.4 F$^2$ in going from 180 down to 47 MeV in the low-energy region, the total cross section of the elementary $\bar{p}N$ interaction increases from 138 to 220 mb.

Taking into account the observation about the partial cancellation of the two corrections, it can be concluded that the impulse approximation for the imaginary part of the OP is fairly accurate for antiprotons with kinetic energy 50–20 MeV. Our analysis shows that the large value of the total cross section for the elementary $\bar{p}N$ interaction, the dominant contribution of the annihilation channel ($\sigma_s/\sigma_t\approx 1/3$), and the small ratio $|\mathrm{Re}\,M_{\bar{p}N}(0)/\mathrm{Im}\,M_{\bar{p}N}(0)|$ favor the use of the GST at low antiproton energies.

## 3. MULTIPLE SCATTERING IN ANTINUCLEON ANNIHILATION ON NUCLEI

### 3.1. Annihilation and quasifree antinucleon scattering

Let us begin our analysis of the role of multiple scattering in the process of antinucleon annihilation on nuclei with the calculation of the contribution of those scattering events which precede annihilation as such.[32,33] We use the familiar expression for the reaction cross section:[104]

$$\sigma_R=-\frac{2}{\hbar v_0}\langle\psi_{\mathbf{k}}^{(+)}|\operatorname{Im} V_{\text{op}}|\psi_{\mathbf{k}}^{(+)}\rangle. \tag{3.1}$$

Here $v_0$ is the relative velocity of the incident particle and the target nucleus, $V_{\text{op}}$ is the optical potential, and $\psi_{\mathbf{k}}^{(+)}(\mathbf{r})$ is the wave function of the incident particle with wave vector $\mathbf{k}$ (in the particle–nucleus c.m. frame, the PT frame) satisfying the wave equation

$$\{\nabla^2+k^2[1-U_{\text{op}}(\mathbf{r})]\}\psi_{\mathbf{k}}^{(+)}(\mathbf{r})=0.$$

The dimensionless OP $U_{\text{op}}(\mathbf{r})$ is defined above [see (2.9)]. Only the central nuclear potential is taken into account. The spin–orbit interaction has a weak effect on the value of the antiproton annihilation cross section, and the Coulomb interaction $V_C$ can be taken into account by including the factor $(1+V_C(R))/(E_{\bar p}+E_A)$; $V_C(R)$ is the value of the Coulomb potential at the surface of the nucleus, and $E_{\bar p}+E_A$ is the sum of the kinetic energies of the incident particle and the nucleus in the PT frame. The Coulomb factor obviously does not enter into the ratio of the partial annihilation cross sections.

The reaction cross section is the sum of terms corresponding to annihilation $\sigma_a$ and inelastic scattering of antiprotons followed by their emission from inside the nucleus $\sigma_{\text{in}}$. We shall ignore the relatively small cross section for charge exchange $\bar p\to\bar n$ and possible pion production. Antiproton annihilation can occur not only in the entrance channel, but also after one or several inelastic collisions resulting in excitation of the target nucleus. Using the standard projection-operator technique, we write down the following expression for the annihilation cross section:

$$\sigma_a=-\frac{2}{\hbar v_0}\operatorname{Im}\langle\Psi^{(+)}(P_0+P_1)|V_{\text{op}}^{P_0+P_1\to Q}|(P_0+P_1)\Psi^{(+)}\rangle. \tag{3.2}$$

Here we have used the notation

$$V_{\text{op}}^{P_0+P_1\to Q}=(P_0+P_1)\hat H Q\frac{1}{E-Q\hat H Q+i\eta}Q\hat H(P_0+P_1). \tag{3.3}$$

The wave function $\Psi^{(+)}$ of the multiparticle problem of the interaction of the incident antiproton with the nucleus satisfies the wave equation

$$(E-\hat H)\Psi^{(+)}=0.$$

The projection operators $P_0$, $P_1$, and $Q$ project the wave function $\Psi^{(+)}$ onto different regions of Hilbert space: $P_0$ projects onto the region corresponding to motion of the antiproton in the field of the nucleus in the ground state $\Phi_0(\mathbf{R}_1,\mathbf{R}_2,\ldots\mathbf{R}_A)$, and $P_1$ projects onto the region of states describing the motion of an antiproton which has undergone one or several inelastic collisions with excitation of the nucleus into the state $\Phi_f(\mathbf{R}_1,\ldots\mathbf{R}_A)$; $\mathbf{R}_1,\ldots\mathbf{R}_A$ are the coordinates of the nucleons in the target nucleus. The operator $Q$ projects $\Psi^{(+)}$ onto the Hilbert space of states which do not contain the antiproton, and the nucleus with mass number $A-1$ is in an excited state.

The isolation of antiprotons from the entrance channel is described by the OP

$$V_{\text{op}}^{P_0\to P_1+Q}=P_0\hat H(P_1+Q)\frac{1}{E-(Q+P_1)\hat H(P_1+Q)+i\eta}\times(P_1+Q)\hat H P_0, \tag{3.4}$$

which, assuming that the propagator $[E-(Q+P_1)\hat H(P_1+Q)+i\eta]^{-1}$ is diagonal in $P_1\Psi^{(+)}$ and $Q\Psi^{(+)}$, can be written as two terms (see Appendix 1):

$$V_a^{P_0\to Q}\underset{\eta\to0}{\cong}P_0\hat H Q\frac{1}{E-Q\hat H Q+i\eta}Q\hat H P_0, \tag{3.5}$$

corresponding to antiproton annihilation as a result of the first collision, and

$$V_{in}^{P_0\to P_1}\underset{\eta\to0}{\cong}P_0\hat H P_1\frac{1}{E-P_1\hat H P_1+i\eta}P_1\hat H P_0, \tag{3.6}$$

describing the processes following the first inelastic scattering of the antiproton. This approximate splitting of the OP corresponds to the reaction content of the first-order OP: $\operatorname{Im}V_{\text{op}}^{(1)}\sim\operatorname{Im}t_{\bar NN}=\operatorname{Im}t_a^{\bar NN}+\operatorname{Im}t_{in}^{\bar NN}$, where $\operatorname{Im}t_a^{\bar NN}\sim\sigma_a^{\bar NN}$ is the antiproton–nucleon annihilation cross section and $\operatorname{Im}t_{in}^{\bar NN}$ corresponds to the cross section for elastic scattering of the antinucleon on a nucleon of the nucleus, $\sigma_{el}^{\bar NN}$. In this approximation the cross section for annihilation as a result of the first interaction of the antiproton with the nucleus takes the form

$$\sigma_a^{(1)}=-\frac{2}{\hbar v_0}\operatorname*{Im}_{\eta\to0}\left\langle\Psi^{(+)}P_0\middle|P_0\hat H Q\frac{1}{E-Q\hat H Q+i\eta}Q\hat H P_0\middle|\times P_0\Psi^{(+)}\right\rangle, \tag{3.7}$$

and the cross section for processes occurring after the first inelastic scattering is

$$\sigma_{in}^{(1)}=-\frac{2}{\hbar v_0}\operatorname*{Im}_{\eta\to0}\left\langle\Psi^{(+)}P_0\middle|P_0\hat H P_1\frac{1}{E-P_1\hat H P_1+i\eta}P_1\hat H P_0\middle|\times P_0\Psi^{(+)}\right\rangle. \tag{3.8}$$

The solution of the wave equation of the optical model with coupled channels, when the states $Q|\Psi^{(+)}\rangle$ are not treated explicitly, can be written in the eikonal approximation. In this approximation the sum of the cross sections for all annihilation processes is $\sigma_a\sim\int d^2b[1-e^{-\varphi_a(b)}]$, where $e^{-\varphi_a(b)}$ is the probability of avoiding annihilation in

motion with impact parameter $b$; $\varphi_a(b) \sim \sigma_a^{\bar{N}N}$. Accordingly, the inelastic scattering cross section is $\sigma_{in} \sim \int d^2b e^{-\varphi_a(b)}[1 - e^{-\varphi_{in}(b)}]$, where $\varphi_{in}(b) \sim \sigma_{el}^{\bar{N}N} = \sigma_t^{\bar{N}N} - \sigma_a^{\bar{N}N}$. It is easily verified that in the EA the total reaction cross section is $\sigma_R = \sigma_a + \sigma_{in} \sim \int d^2b[1 - e^{-\varphi_a(b)-\varphi_{in}(b)}]$. Here the cross section for annihilation as a result of the first collision is

$$\sigma_{a\,\mathrm{EA}}^{(1)} = \frac{\sigma_a^{\bar{N}N}}{\sigma_a^{\bar{N}N} + \sigma_{el}^{\bar{N}N}} \sigma_{R\,\mathrm{EA}}, \tag{3.9}$$

and the cross section for processes following after the first inelastic scattering event is

$$\sigma_{in\,\mathrm{EA}}^{(1)} = \frac{\sigma_{el}^{\bar{N}N}}{\sigma_a^{\bar{N}N} + \sigma_{el}^{\bar{N}N}} \sigma_{R\,\mathrm{EA}}. \tag{3.10}$$

Obviously, $\sigma_{R\,\mathrm{EA}} = \sigma_{in\,\mathrm{EA}}^{(1)} + \sigma_{a\,\mathrm{EA}}^{(1)}$. Equations (3.9) and (3.10) are also satisfied outside the EA: it is necessary that Im $V_a$ and Im $V_{in}$ have the same spatial dependence. The cross section $\sigma_{in}^{(1)}$ contains the contribution of those annihilation processes which occurred after the first, second, etc. inelastic scattering event. Here

$$\Delta\sigma_a = \sigma_{a\,\mathrm{EA}} - \sigma_{a\,\mathrm{EA}}^{(1)} = \sigma_{a\,\mathrm{EA}} - \frac{\sigma_a^{\bar{N}N}}{\sigma_a^{\bar{N}N} + \sigma_{el}^{\bar{N}N}} \sigma_{R\,\mathrm{EA}}. \tag{3.11}$$

The simple expressions given above are valid when $\sigma_a^{\bar{N}N}$ and $\sigma_{el}^{\bar{N}N}$ depend weakly on the energy.

In order to separate explicitly the cross section for annihilation immediately after the first inelastic scattering event, it is necessary to find the wave function $P_{11}|\Psi^{(+)}\rangle$ from the subspace $P_1|\Psi^{(+)}\rangle$ describing the motion of the antiproton after the first inelastic scattering event in the field of the excited target nucleus. Taking into account only the direct coupling between the states $P_0|\Psi^{(+)}\rangle$ and $P_{11}|\Psi^{(+)}\rangle$, by the usual procedure we obtain

$$\begin{aligned}\psi_2 &= \left[E + i\eta - H_{22} - H_{23}\frac{1}{E + i\eta - H_{33}} H_{31}\right]^{-1} \\ &\times \left[H_{21} + H_{23}\frac{1}{E + i\eta - H_{33}} H_{31}\right]\psi_1 \\ &\approx \left[E + i\eta - H_{22} - H_{23}\frac{1}{E + i\eta - H_{33}} H_{32}\right]^{-1} H_{21}\psi_1.\end{aligned} \tag{3.12}$$

Here to condense the notation we have used

$$P_0|\Psi^{(+)}\rangle = \psi_1, \quad Q|\Psi^{(+)}\rangle = \psi_3, \quad P_{11}|\Psi^{(+)}\rangle = \psi_2,$$

$$P_0\hat{H}P_0 = H_{11}, \quad P_1\hat{H}P_0 = H_{21}, \quad Q\hat{H}P_0 = H_{31}, \quad \text{etc.}$$

The cross sections for annihilation as a result of the first interaction of the antiproton with the nucleus $\sigma_a^{(1)}$ and after a single inelastic scattering event $\sigma_a^{(2)}$ can be written as (see Appendix 1)

$$\sigma_a^{(1)} = -\frac{2}{\hbar v_0} \mathrm{Im}\left\langle \psi_1 \middle| H_{13}\frac{1}{E + i\eta - H_{33}} H_{31} \middle| \psi_1 \right\rangle \tag{3.13}$$

and

$$\sigma_a^{(2)} = -\frac{2}{\hbar v_0} \mathrm{Im}\left\langle \psi_2 \middle| H_{23}\frac{1}{E + i\eta - H_{33}} H_{32} \middle| \psi_2 \right\rangle. \tag{3.14}$$

In Eq. (3.14) there is understood to be a summation over the excited states of the nucleus $f$. In the case of the nuclear model of independent particles this operation reduces to summation over excited states of the type $1p1h$ (one particle–one hole). If the values of $\sigma_a^{(1)}$, as shown above, can be obtained by the standard optical-model calculation, then calculations using (3.14) require additional simplifications. Let us write down $\psi_2$ (3.12) in the coordinate representation, after explicitly separating out the index $f$ labeling the excited state of the nucleus:

$$\begin{aligned}\psi_{2f}(\mathbf{r}) = \int d\mathbf{r}'d\mathbf{r}''d\mathbf{R}_1 \ldots d\mathbf{R}_A G_{\mathrm{op}}^{(2f)}(\mathbf{r};\mathbf{r}')\Phi_f^*(\mathbf{R}_1,\ldots,\mathbf{R}_A) \\ \times \sum_{j=1}^{A} t^{\bar{N}N}(\mathbf{r}',\mathbf{r}'',\{\mathbf{R}_j\})\Phi_0(\mathbf{R}_1,\ldots\mathbf{R}_A)\tilde{\psi}_1(\mathbf{r}'').\end{aligned} \tag{3.15}$$

Here $G_{\mathrm{op}}^{(2f)}(\mathbf{r};\mathbf{r}')$ [in the coordinate representation $G_{\mathrm{op}}^{2f} = [E + i\eta - H_{22}^f - V_a^{2f}]$] is the propagator of the antiproton in the field of the nucleus in the excited state $f$, and $\tilde{\psi}_1$ is the solution of the optical-model wave equation for the entrance channel with the contribution of inelastic scattering excluded from the OP. In addition, $t^{\bar{N}N}(\mathbf{r},\mathbf{r}',\{\mathbf{R}_j\})$ is the $t$ matrix for antiproton scattering on a nucleon bound in the target nucleus. In the following calculations we shall take $t^{\bar{N}N}(\mathbf{r},\mathbf{r}',\{\mathbf{R}_j\})$ to be the $t$ matrix for antiproton scattering on a free nucleon (the impulse approximation). In obtaining (3.15) we used the relation (see Appendix 1)

$$\begin{aligned}\int d\mathbf{r}' \sum_{j=1}^{A} v_j^{\bar{N}N}(\mathbf{r},\mathbf{r}';\{\mathbf{R}_j\})\Phi_0(\mathbf{R}_1,\ldots\mathbf{R}_A)\psi_1(\mathbf{r}) \\ = \int d\mathbf{r}' \sum_{j=1}^{A} t^{\bar{N}N}(\mathbf{r},\mathbf{r}';\{\mathbf{R}_j\}\Phi_0(\mathbf{R}_1,\ldots\mathbf{R}_A)\tilde{\psi}_1(\mathbf{r}'),\end{aligned}$$

where $v^{\bar{N}N}(\mathbf{r},\mathbf{r}'\{\mathbf{R}_j\})$ is the potential generating the $t$ matrix $t^{\bar{N}N}(\mathbf{r},\mathbf{r}'\{\mathbf{R}_j\})$. We use the local forms of $v$ and $t$, where

$$H_{21}\psi_1(\mathbf{r}) = \sum_{j=1}^{A} t_j^{\bar{N}N}\tilde{\psi}_1(\mathbf{r}). \tag{3.16}$$

We write (3.15) in terms of the transition density

$$\begin{aligned}\rho_{f0}(\mathbf{r}) = \frac{1}{A}\sum_{j=1}^{A}\int d\mathbf{R}_1,\ldots d\mathbf{R}_A\Phi_f^*(\mathbf{R}_1,\ldots\mathbf{R}_A) \\ \times\delta(\mathbf{r} - \mathbf{R}_j)\Phi_0(\mathbf{R}_1,\ldots\mathbf{R}_A),\end{aligned} \tag{3.17}$$

and

$$\begin{aligned}\psi_{2f}(\mathbf{r}) = A\int d\mathbf{r}'d\mathbf{r}''G_{\mathrm{op}}^{(2f)}(\mathbf{r}|\mathbf{r}')t^{\bar{N}N}(\mathbf{r}' - \mathbf{r}'') \\ \times\tilde{\psi}_1(\mathbf{r}')\rho_{f0}(\mathbf{r}'').\end{aligned} \tag{3.18}$$

The Green function $G_{\mathrm{op}}^{(2f)}(\mathbf{r};\mathbf{r}'')$ is calculated at the energy of the singly scattered antiproton, and $t^{\bar{N}N}$ and $\tilde{\psi}_1$ are calculated at the energy of the incident $\bar{p}$. We substitute

TABLE III. Values of the parameter $R$, F.

| Energy, MeV / Nucleus | 50 | 100 | 200 | 300 | 500 | 1000 | 2000 |
|---|---|---|---|---|---|---|---|
| $^{20}$Ne | 0,497 (0,385) | 0,602 (0,470) | 0,72 (0,557) | 0,781 (0,607) | 0,843 (0,665) | 0,897 (0,732) | 0,936 (0,787) |
| $^{64}$Cu | 0,696 (0,525) | 0,849 (0,641) | 1,026 (0,763) | 1,121 (0,835) | 1,219 (0,921) | 1,314 (1,030) | 1,387 (1,125) |
| $^{208}$Pb | 1,009 (0,746) | 1,232 (0,910) | 1,496 (1,085) | 1,641 (1,189) | 1,794 (1,318) | 1,947 (1,485) | 2,071 (1,639) |

The values of $R$ given in parentheses were obtained using (3.27), where $\sigma_a$ and $\mathrm{Im}U_{a(1)}(0)$ are replaced by $\sigma_R$ and $\mathrm{Im}U^{(1)}_{a+\mathrm{in}}(0)$, respectively.

(3.18) into (3.14) and sum over $f$ in the convolution approximation, where all excited states of the nucleus are assumed to be equivalent to a single degenerate state with excitation energy $\langle\Delta\varepsilon\rangle$. Assuming that the target nucleus is of large extent, so that $G^{(2f)}_{\mathrm{op}}(\mathbf{r};\mathbf{r}') \approx G^{(2f)}_{\mathrm{op}}(\mathbf{r}-\mathbf{r}')$ and $\int d\mathbf{r}e^{i\mathbf{q}\mathbf{r}}\mathrm{Im}\,U^{(2)}_{\mathrm{op}}(\mathbf{r}) \approx (2\pi)^3\mathrm{Im}U^{(2)}_a(0)\delta(\mathbf{q})$, and using (A27), we obtain

$$\sigma^{(2)}_a=-\frac{k_2}{k_1}k_2\,\mathrm{Im}\,U^{(2)}_a(0)A\int\frac{d\mathbf{s}}{(2\pi)^3}|g^{(2)}_{\mathrm{op}}(\mathbf{s})|^2\int\frac{d\mathbf{q}}{(2\pi)^3}\times\int\frac{d\mathbf{q}'}{(2\pi)^3}\tau^{\bar{N}N}(\mathbf{q})\tau^{\bar{N}N*}(\mathbf{q}')\tilde{\varphi}_1(\mathbf{s}-\mathbf{q}')\tilde{\varphi}^*_1(\mathbf{q}'-\mathbf{s}). \tag{3.19}$$

We have introduced the notation

$$\tilde{\varphi}_1(\mathbf{s})=\int\tilde{\psi}_1(\mathbf{r})e^{i\mathbf{s}\mathbf{r}}d\mathbf{r};\quad \tau^{\bar{N}N}(\mathbf{q})=\int t^{\bar{N}N}(\mathbf{r})e^{i\mathbf{q}\mathbf{r}}d\mathbf{r}$$

and

$$g^{(2)}_{\mathrm{op}}(\mathbf{s})=\int G^{(2)}_{\mathrm{op}}(\mathbf{r})e^{i\mathbf{s}\mathbf{r}}d\mathbf{r}.$$

Here $\mathbf{k}_1$ and $\mathbf{k}_2$ are the wave vectors of the incident and singly scattered antiprotons $\{k_2=k_2(E_{\bar{p}}-\langle\Delta\varepsilon\rangle)\}$, and $U^{(2)}_a(0)$ is the value of the annihilation component of the OP at the center of the nucleus at energy $E_{\bar{p}}-\langle\Delta\varepsilon\rangle$.

The expression (3.19) that we have obtained is still too complicated for calculations. We shall therefore simplify it by means of the commonly used distorted-wave approximation for $\tilde{\psi}_1$ (Refs. 105–109):

$$\tilde{\psi}_1(\mathbf{r})=e^{i\mathbf{k}_1\mathbf{r}}e^{-i(k_1R/2)U^{(1)}_a(0)}. \tag{3.20}$$

Here $U^{(1)}_a(0)$ is the value of the annihilation component of the dimensionless OP at the center of the nucleus at the energy of the incident antiproton, and $R$ is the depth to which the incident wave penetrates inside the nucleus—an effective parameter subject to definition. Equation (3.19) simplifies considerably in the approximation (3.20):

$$\sigma^{(2)}_a=-\frac{k_2}{k_1}k_2\,\mathrm{Im}\,U^{(2)}_a(0)Ae^{Rk\,\mathrm{Im}\,U^{(1)}_a(0)}\times\int\frac{d\mathbf{s}}{(2\pi)^3}|g^{(2)}_{\mathrm{op}}(\mathbf{s})|^2|\tau^{\bar{N}N}(\mathbf{k}_1+\mathbf{s})|^2. \tag{3.21}$$

The structure of this expression obviously differs from the result of the classical calculation:

$$\int\frac{d\sigma^{\bar{N}N}_{el}(k_1)}{d\Omega}d\Omega\int\hat{G}_{\mathrm{cl}}(\mathbf{r})|\tilde{\psi}_1(\mathbf{r})|^2d\mathbf{r},$$

where $\hat{G}_{\mathrm{cl}}(\mathbf{r})$ is the Green function of the classical transport equation. In the spirit of the approximation (3.20) we write

$$G^{(2)}_{\mathrm{op}}(\mathbf{r}-\mathbf{r}')=\frac{1}{4\pi|\mathbf{r}-\mathbf{r}'|}\exp(ik_2|\mathbf{r}-\mathbf{r}'|-\gamma_2|\mathbf{r}-\mathbf{r}'|), \tag{3.22}$$

$$\gamma_2=|k_2\,\mathrm{Im}\,U^{(2)}_a(0)|/2 \tag{3.23}$$

and

$$g_2(s)=(s^2-k_2^2+\gamma_2^2-2ik_2\gamma_2)^{-1} \tag{3.24}$$

and use the standard parametrization of the dependence of $\tau^{\bar{N}N}(q)$ on the momentum transfer $q$,

$$\tau^{\bar{N}N}(q)=\tau_0e^{-\beta q^2/2}, \tag{3.25}$$

and after integrating over angles $d\Omega_{\mathbf{s}}$ we obtain the final expression for $\sigma^{(2)}_a(k_1)$:

$$\sigma^{(2)}_a(k_1)=-\frac{k_2}{k_1}k_2A\frac{\mathrm{Im}\,U^{(2)}_a(0)}{(2\pi)^2}e^{k_1R\,\mathrm{Im}\,U^{(1)}_a(0)}|\tau_0|^2\frac{e^{-\beta k_1^2}}{2\beta k_1}\times\int_0^\infty\frac{qdqe^{-\beta q^2}[e^{2\beta qk_1}-e^{-2\beta qk_1}]}{(q^2-k_2^2+\gamma_2^2)^2+4\gamma_2^2k_2^2}. \tag{3.26}$$

The values of the parameters $\sigma^{\bar{N}N}_t$, $\sigma^{\bar{N}N}_a$, $\beta$, and $\alpha=\mathrm{Re}\,M^{\bar{N}N}(0)/\mathrm{Im}\,M^{\bar{N}N}(0)$ used in the actual calculations were taken from Refs. 1, 23, 76, 50, and 110. The free parameter $R$ is determined from the condition that $\sigma_a$ calculated using the approximation (3.20) for $\tilde{\psi}_1$ coincides with the annihilation cross section calculated in the EA without use of (3.20):

$$R=\frac{1}{|k_1\,\mathrm{Im}\,U^{(1)}_a(0)|}\left|\ln\frac{\sigma_a(k_1)}{|k_1\,\mathrm{Im}\,\hat{U}^{(1)}_a(0)|}\right|. \tag{3.27}$$

TABLE IV. Values of the slope parameter of the $\bar{N}N$-scattering amplitude $\beta$ and $\langle\Delta\varepsilon\rangle=\hbar^2/2M\beta$.

| Energy, MeV | 50 | 100 | 200 | 300 | 500 | 1000 | 2000 |
|---|---|---|---|---|---|---|---|
| $\beta$, F$^2$ | 1,343 | 1,003 | 0,757 | 0,655 | 0,571 | 0,512 | 0,478 |
| $\langle\Delta\varepsilon\rangle$,MeV | 15,45 | 20,69 | 27,40 | 31,68 | 36,34 | 40,53 | 43,41 |

The quantity $\hat{U}_a^{(1)}(0)$ when the WS form is used is related to the value of the annihilation OP at the center of the nucleus $U_a^{(1)}(0)$ as

$$\hat{U}_a^{(1)}(0)=U_a^{(1)}(0)\,\frac{4\pi R_{ef}^3}{3}\left[1+\left(\frac{\pi a_{ef}}{R_{ef}}\right)^2\right]\frac{1}{1+e^{-R_{ef}/a_{ef}}}. \tag{3.28}$$

The effective parameters $R_{ef}$ and $a_{ef}$ are defined above [see (2.14)]. The values of the parameter $R$ are given in Table III.

The average energy transferred in a quasifree collision of the incident antiproton with an intranuclear nucleon is the following for the Gaussian parametrization of the $\bar{N}N$ scattering amplitude that we are using:

$$\langle\Delta\varepsilon\rangle\approx\frac{\hbar^2\langle q^2\rangle}{2M_N}=\frac{\hbar^2}{2M_N\beta}. \tag{3.29}$$

Since the first inelastic collision of the antiproton with the nucleus is peripheral in nature, in accordance with the discussion in Sec. 2.6 we have neglected the effect of the Pauli principle on the value of the energy transferred from the antinucleon to the nucleus. The values of $\langle\Delta\varepsilon\rangle$ at different antiproton energies $E_{\bar{p}}$ are given in Table IV. In the range of $E_{\bar{p}}$ under consideration, when calculating $\langle\Delta\varepsilon\rangle$ it is very important to include the anisotropy of $\bar{N}N$ scattering. We recall that when $\bar{N}N$ scattering is isotropic in the c.m. frame we have $\langle\Delta\varepsilon\rangle\approx E_{\bar{p}}/2$ in the nonrelativistic approximation. The inclusion of relativistic corrections in the calculation of $\langle\Delta\varepsilon\rangle$ for energies up to 1.0 GeV has little effect on the results.

The results of the calculations of $\sigma_a^{(1)}$, $\sigma_a^{(2)}$, $\sigma_a$, and $\sigma_R$ for antiproton interactions with $^{20}$Ne, $^{64}$Cu, and $^{208}$Pb nuclei are shown in Figs. 12–14. There we also give the curves for $\Delta\sigma_a=\sigma_a-\sigma_a^{(1)}$, the cross section for annihilation coming from all excited states of the target nucleus. The energy dependence of the cross sections $\sigma_R$, $\sigma_a$, $\sigma_a^{(1)}$, and $\Delta\sigma_a$ calculated using the EA expressions on the whole mimic the energy behavior of the cross sections $\sigma_t^{\bar{N}N}$ and $\sigma_a^{\bar{N}N}$ for antinucleon–nucleon collisions. Meanwhile, $\sigma_a^{(2)}$, which remains practically constant in the range 0.3–1.0 GeV, decreases slowly for $E_{\bar{p}}>1.0$ GeV and rapidly for $E_{\bar{p}}<0.3$ GeV: $\sigma_a^{(2)}/\sigma_a^{(1)}\approx 0.25$–$0.3$ for $E_{\bar{p}}=0.3$–$1.0$ GeV for all nuclei and reaches 0.05 for $E_{\bar{p}}=0.05$ GeV. The cross section $\sigma_a^{(2)}$ is very sensitive to the values of the slope parameter $\beta$ of the $\bar{N}N$ amplitude. The energy dependence of $\sigma_a^{(2)}$ arises mainly from the form of $\beta(E_{\bar{p}})$. The cross section $\sigma_a^{(2)}$ is the inclusive annihilation cross section for all antiprotons which have undergone at least one inelastic collision. We define the exclusive annihilation cross section $\sigma_a^{(21)}$ for antiprotons which have undergone one (and only one!) inelastic collision using the expression for $\sigma_a^{(2)}$, in which $\gamma_2$ is proportional to the imaginary part of the total OP, and not only to the annihilation component. The energy dependence of $\sigma_a^{(21)}$ mimics that of $\sigma_a^{(2)}$ and for the $^{20}$Ne, $^{64}$Cu, and $^{208}$Pb nuclei is $\sim 0.5\sigma_a^{(2)}$ in the energy range in question. The total inclusive annihilation cross section $\sigma_a$ is the sum of all the exclusive cross sections $\sigma_a=\sigma_a^{(1)}+\sigma_a^{(21)}+\sigma_a^{(22)}+\ldots$. In Table V we give the results of calculations of $\Delta\sigma_a/\sigma_a^{(1)}$ and $\sigma_a^{(2)}/\sigma_a^{(1)}$ for $\bar{p}^{20}$Ne, $\bar{p}^{64}$Cu,

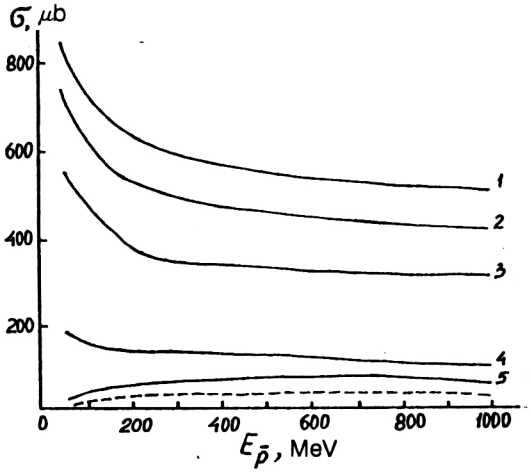


FIG. 12. Energy dependence of the reaction cross section $\sigma_R$ (curve *1*) and the annihilation cross sections $\sigma_a$ (curve *2*), $\sigma_a^{(1)}$ (curve *3*), $\Delta\sigma_a$ (curve *4*), and $\sigma_a^{(2)}$ (curve *5*) for antiproton interactions with $^{20}$Ne. The dashed line is $\sigma_a^{(21)}$ calculated using Eq. (3.26), where the values of the parameter $\gamma_2$ are determined by the complete OP $U^{(2)}$.

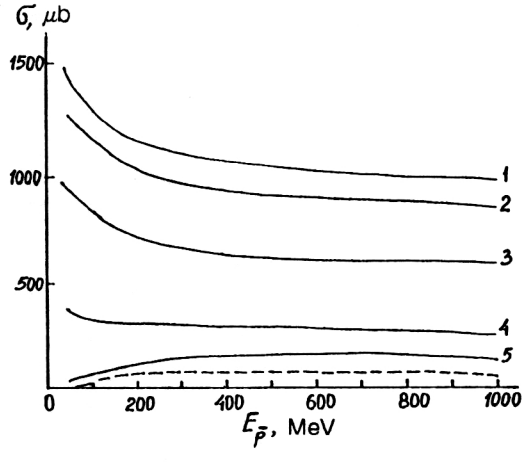


FIG. 13. The same as in Fig. 12 for $\bar{p}^{64}$Cu.

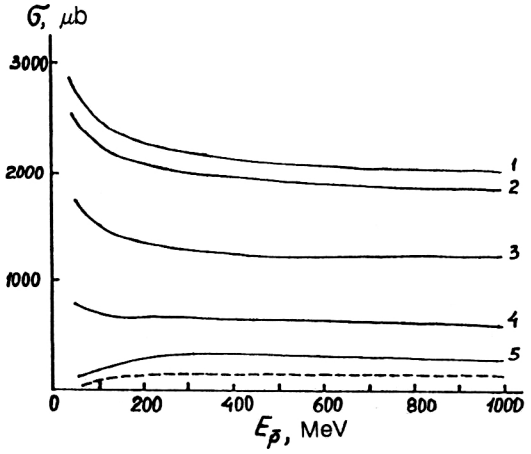


FIG. 14. The same as in Fig. 12 for $\bar{p}^{208}$Pb.

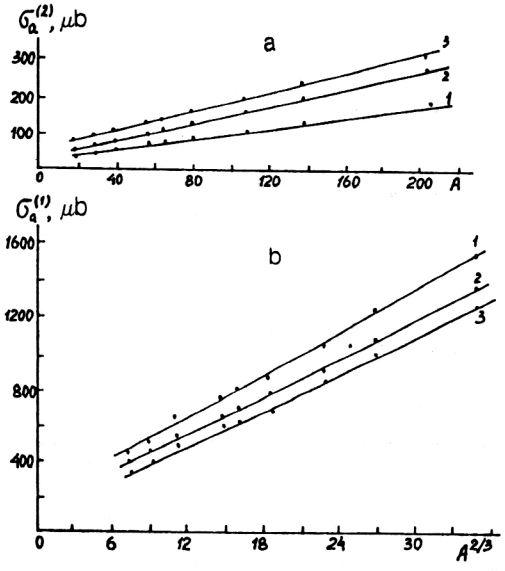


FIG. 15. The $A$ dependence of the cross sections $\sigma_a^{(2)}$ (a) and $\sigma_a^{(1)}$ (b). Curves *1–3* respectively correspond to the incident-antiproton kinetic energy equal to 100, 200, and 1000 MeV.

and $\bar{p}^{208}$Pb interactions, and $\xi$, the ratio of the number of antiproton annihilation events inside the nucleus to the number at the nuclear surface for $\bar{p}^{20}$Ne interactions and antiproton interactions with Ag and Br nuclei in emulsion.[31] We see that $\Delta\sigma_a/\sigma_a^{(1)}$ and $\sigma_a^{(2)}/\sigma_a^{(1)}$ are the same quantity, calculated using directly opposed models of the interaction between antiprotons and intranuclear nucleons[33] and that they are the upper and lower limits of $\xi$. The use in the calculation of $\sigma_a^{(2)}$ of the values of the parameter $R$ found from the reaction cross sections (the values of $R$ in parentheses in Table III) makes the experimentally determined values of $\sigma_a^{(2)}/\sigma_a^{(1)}$ and $\xi$ somewhat closer (by 20–40%). We note that the values of $\xi$ found as the ratio $\sigma_a^{(2)}/\sigma_a^{(1)}$ must be smaller than those obtained experimentally, because the latter include the small contribution from antiproton annihilations inside the nucleus, without any previous inelastic collisions. Therefore, the results for the cross sections $\sigma_a^{(2)}$, $\sigma_a^{(1)}$, and $\Delta\sigma_a$ turn out to be close to the estimates obtained from analysis of the experimental data,[31] in spite of the approximate nature of the calculation and the uncertainty in the analysis carried out in Ref. 31.

The $A$ dependence of the cross sections $\sigma_a^{(1)}$ and $\sigma_a^{(2)}$ is shown by the curves in Fig. 15. The values of $\sigma_a^{(1)}$ are best described by a linear dependence on $A^{2/3}$, while $\sigma_a^{(2)} \sim A$, which corresponds to the predominantly surface nature of the interaction in the first case and the volume nature of the interaction in the second.

### 3.2. Dynamics of particles produced in antinucleon annihilation in a nucleus

Here we shall consider the final-state interaction, i.e., the interaction of the particles produced as a result of an-

TABLE V. Calculated values of $\Delta\sigma_a/\sigma_a^{(1)}$ and $\sigma_a^{(2)}/\sigma_a^{(1)}$ and experimental values of the ratio $\xi$ (the ratio of the number of annihilations inside the nucleus and the number of annihilations at the surface) (Ref. 31).*

| Antiproton momentum, MeV/$c$ | | 200 | 300 | 400 | 490 | 600 | 1400 |
|---|---|---|---|---|---|---|---|
| Antiproton energy, MeV | | 20 | 50 | 80 | 120 | 180 | 800 |
| $\Delta\sigma_a/\sigma_a^{(1)}$ | Ne | | 0,34 | 0,33 | 0,33 | 0,36 | 0,38 |
| | Cu | | 0,38 | 0,39 | 0,40 | 0,41 | 0,44 |
| | Pb | | 0,43 | 0,45 | 0,46 | 0,50 | 0,52 |
| $\sigma_a^{(2)}/\sigma_a^{(1)}$ | Ne | | 0,05 (0,07) | 0,07 (0,09) | 0,11 (0,14) | 0,15 (0,20) | 0,25 (0,30) |
| | Cu | | 0,06 (0,10) | 0,09 (0,14) | 0,12 (0,18) | 0,16 (0,24) | 0,26 (0,36) |
| | Pb | | 0,07 (0,14) | 0,10 (0,18) | 0,14 (0,24) | 0,18 (0,32) | 0,27 (0,43) |
| $\xi_{Ne}$ | | 0,15 | | | | 0,25 | |
| $\xi_{Ag/Br}$ | | 0,33 | 0,35 | 0,37 | 0,39 | | 0,59 |

The values of $\sigma_a^{(2)}/\sigma_a^{(1)}$ obtained for the ($R$) in Table I are given in parentheses.

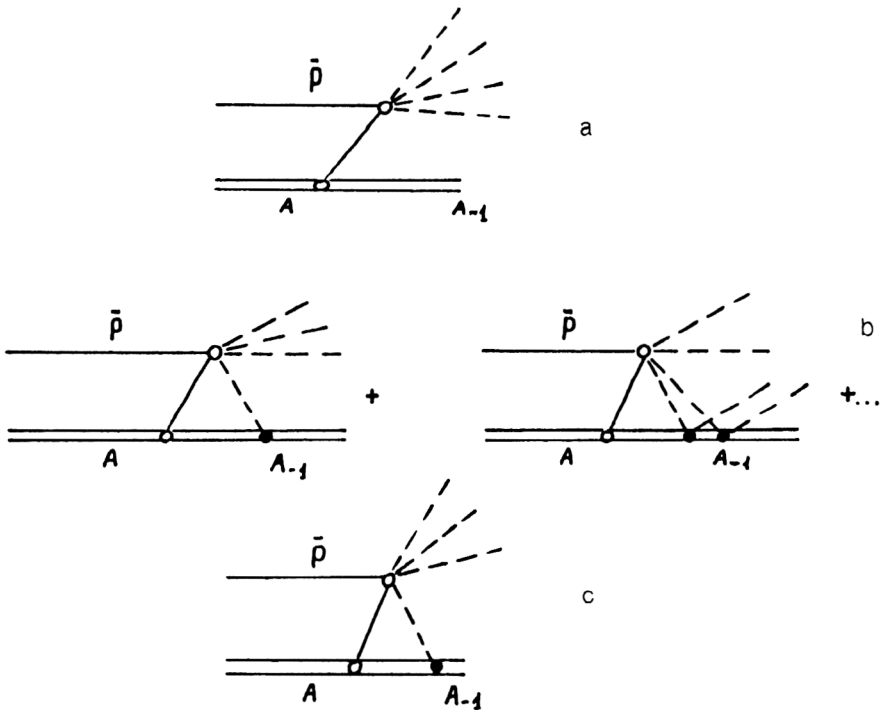


FIG. 16. Diagrams for reactions $\bar{p}A \to n\pi(A-1)$.

nihilation of an antinucleon in the nucleus. Whereas in the preceding subsection we dealt with integrated, inclusive characteristics of the annihilation process, now we must discuss this problem in more detail. The most informative computational technique (informative in the sense that it deals most broadly with the various characteristics of this process) is the intranuclear-cascade (INC) method (Refs. 111–117), in spite of a number of restrictions which significantly narrow its range of applicability. Using this approach, it is possible to obtain the energy and angular distributions of $\pi$, $\eta$, and $\omega$ mesons produced in the annihilation of antinucleons in the nucleus,[118] and of the secondary particles (nucleons, $d$, $^3$He, $^4$He, and so on) which leave the volume of the target nucleus during the development of the INC. In particular, $\eta$ and $\omega$ mesons produced in the annihilation process can be absorbed in the nuclear volume. The contribution of the high-energy nucleons emitted by the nucleus as a result of this event can, in principle, be isolated from the energy and angular distributions of the secondary particles. Therefore, the process of antinucleon annihilation in a nucleus is a source of information on the correlations of nucleons at short distances ($\sim$0.2–0.3 F) located near the nuclear surface. The INC method makes it possible not only to obtain information on such simple characteristics of the annihilation process as the distribution of annihilation events throughout the volume of the nucleus, but also to calculate the probabilities of exotic processes like those studied in Ref. 119, or processes in which antinucleons undergo annihilation on several nucleons of the target nucleus (Refs. 25, 120, and 121). However, the essentially classical INC method is limited in a number of applications.

It is possible to obtain a more detailed microscopic description using quantum-mechanical methods. Since the main products of the $\bar{N}N$ annihilation process are pions, the question of the final-state interaction reduces to the question of pion interactions with the nucleons of the residual nucleus. Compared with the well studied problem of pion scattering by nuclei, we now have the problem of pion sources filling the volume of the nucleus in accordance with the probability distribution for antinucleon annihilation. Therefore, along with the pole diagram (Fig. 16a) we must include both the diagram describing the rescattering of the created mesons (Fig. 16b) and the diagram including the absorption of these mesons (Fig. 16c; Refs. 122–124). The possibility of isolating the contribution of diagrams 16b and 16c by analyzing the energy spectra of the spectator protons in antiproton annihilation on the deuteron has been discussed in Refs. 123 and 124.

As a rule, in calculations some version of the $\Delta h$ (isobar–hole) model is used to describe the passage of pions through nuclear matter. The application of the results of such calculations to specific nuclei involves the local-density approximation. The end products of such calculations are the angular and energy distributions of the pions and nucleons leaving the nucleus, which can have interacted previously with other nucleons of the nucleus (Refs. 125–127). In particular, it has been shown in these studies that, owing to the mechanism of quasifree collisions of annihilation pions with intranuclear nucleons, a significant fraction of the energy released in $\bar{N}N$ annihilation is transferred to the latter.

Analysis of the dynamics of annihilation pions makes it possible to interpret pion rescattering processes as a constituent part of the actual antinucleon annihilation event occuring with the participation of several nucleons, i.e., to describe the annihilation event in terms of exchange currents in the nucleus. Diagrams illustrating this point of view are shown in Fig. 17. In Fig. 18 we show the diagrams describing the complex process of antinucleon annihilation

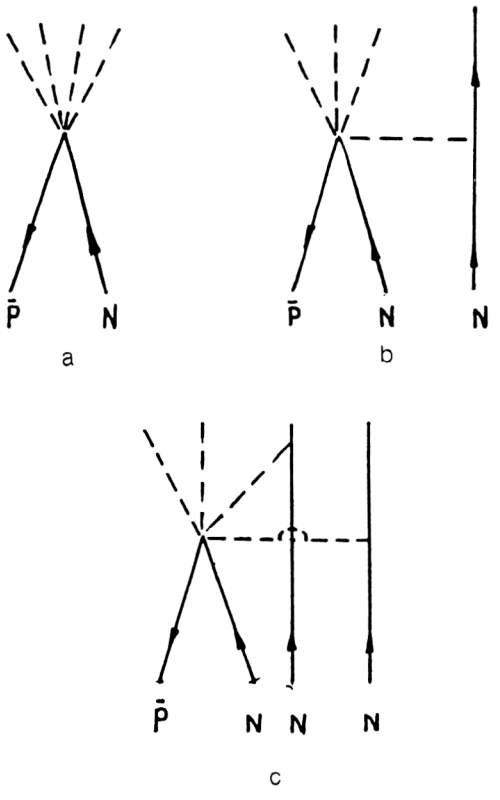


FIG. 17. Diagrams for $\bar{p}N$ annihilation: (a) the standard process $\bar{p}N \to n\pi$; (b) the two-nucleon mechanism with a single off-shell pion; (c) the three-nucleon mechanism with two off-shell pions.

on two intranuclear nucleons in the language of quark dynamics. Since annihilation processes mainly occur on the nuclear surface, the contributions of nuclear configurations with multiple particle–hole excitations decrease with increasing number of excited quasiparticles. As was shown in the preceding subsection, a significant fraction of annihilation processes occurring inside the nucleus can be interpreted in terms of preliminary rescattering of the antinucleon (initial-state interaction) without resorting to the more complex mechanisms discussed in this subsection. The proving ground for studying such nonstandard mechanisms must be reactions in which the multiparticle mechanism dominates: $\bar{p}d \to \pi d$, $\bar{p}A \to \pi(A-1)$, mesonless Pontecorvo reactions $\bar{p}^3\mathrm{He} \to np$, $\bar{p}t \to nn$, and reactions with strange-particle production. The multiparticle annihilation mechanism can be used to explain the discrepancies in the experimental spectra of protons emitted from the nucleus

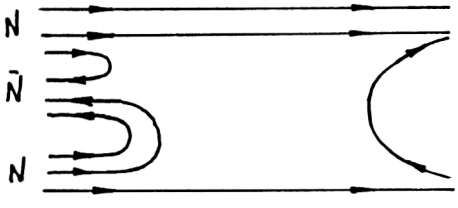


FIG. 18. Quark diagram of antiproton annihilation on two nucleons.

and the spectra calculated in models with a single-particle annihilation mechanism.

In recent years the effect of the nuclear medium on the nature of an individual interaction of an incident hadron $h$ with an intranuclear nucleon has been analyzed at a level more detailed (more "microscopic") than in the method of the Bruckner–Goldstone $g$ matrix for the $hN$ interaction. The effect of the nuclear medium on meson exchange currents has been described using effective meson and nucleon masses inside the nucleus (Refs. 128–131). Such a renormalization of the meson masses in a nuclear medium modifies the meson dispersion law and deforms the region of phase space accessible in the reaction. This can, in particular, lead to several observable effects in antinucleon annihilation on nuclei.[132] The effect of the nuclear medium on annihilation in nuclear matter is, however, small because of the large energy release in this process, and also because the annihilation of incident antinucleons occurs mainly at the periphery of the nucleus where the nuclear density is low. In some cases it is important to include the interaction between the mesons created in the $\bar{N}N$ annihilation process,[133] and the effect of the nuclear medium on this interaction.[134]

## 4. CONCLUSION

In this review we have discussed the effects of the multiple scattering of intermediate-energy antinucleons when they interact with nuclei. Among the questions touched upon are the analysis of the manifestations of these effects in the most probable interaction processes: in elastic scattering and annihilation. The angular distributions of elastically scattered antinucleons can be described phenomenologically using some model of strong absorption. At intermediate and low incident-antinucleon energies the depth to which these particles penetrate into the nucleus is $\sim 1$ F, and the characteristics of the antinucleon–nucleus interaction are mainly determined by the collisions between antinucleons and nucleons in the peripheral region of the target nucleus. This tends to weaken the effects of the nuclear medium in interactions of antinucleons with nucleons bound inside the nucleus, and the theoretical methods which have been widely used to describe nucleon interactions with nuclei at considerably higher energies ($\gtrsim 1$ GeV) have turned out to be very effective. The most important such method is the Glauber–Sitenko theory.

It follows from this analysis of antiproton annihilation on nuclei during the early stages of their interaction with intranuclear nucleons that most of the annihilation cross section $\sigma_a$ ($\gtrsim 2/3$) comes from $\sigma_a^{(1)}$, the cross section for antinucleon annihilation in the entrance channel, and annihilation occurs mainly on the surface of the target nucleus. The rest of the cross section $\sigma_a$ is mainly related to those annihilation processes occurring after the antinucleon, having undergone a quasifree collision with a nucleon at the nuclear surface, penetrates into the region of denser nuclear matter in the central part of the target nucleus.

The problems discussed here have not been treated in

equal detail, owing to lack of space and the scientific interests of the authors.

## APPENDIX 1

The total annihilation cross section is determined by the flux of annihilation products, i.e., the flux related to transitions of states from the $P_0+P_1$ subspace to a state in the $Q$ subspace. The projection of $|\Psi^{(+)}\rangle$ onto the $P_0+P_1$ subspace satisfies the equation

$$\left\{E-\left[(P_0+P_1)\hat{H}(P_0+P_1)+(P_0+P_1)\hat{H}\frac{1}{E-Q\hat{H}Q+i\eta}\right.\right.$$
$$\left.\left.\times Q\hat{H}(P_0+P_1)\right]\right\}(P_0+P_1)|\Psi^{(+)}\rangle=0, \quad \text{(A1)}$$

$\eta\to+0$; $E$ is the total energy of the antinucleon–nucleus system. We write

$$\hat{H}=(P_0+P_1+Q)\hat{H}(P_0+P_1+Q)$$
$$=(P_0+P_1)\hat{H}(P_0+P_1)+Q\hat{H}Q+(P_0+P_1)\hat{H}Q$$
$$+Q\hat{H}(P_0+P_1)$$
$$\equiv\hat{H}_1+\hat{H}_2, \quad \text{(A2)}$$

where $\hat{H}_1=(P_0+P_1)\hat{H}(P_0+P_1)+Q\hat{H}Q$, and $\hat{H}_2=Q\hat{H}(P_0+P_1)+(P_0+P_1)\hat{H}Q$ describes antinucleon creation and annihilation.

Let us split $H_1$ into components:

$$\hat{H}_1=\hat{H}_1'+\hat{H}_1'';$$
$$\hat{H}_1'=P_0\hat{H}P_0+P_1\hat{H}P_1+Q\hat{H}Q, \quad \text{(A3)}$$
$$\hat{H}_1''=P_0\hat{H}P_1+P_1\hat{H}P_0 \quad \text{(A4)}$$

describes antinucleon inelastic scattering (without going to states of the $Q$ subspace).

Summing the squared moduli of the matrix elements of transitions from states $a$ ($P_0+P_1$ subspace) to any state $b$ ($Q$ subspace)

$$\langle b|T|a\rangle=\langle\chi_b^{(-)}|Q\hat{H}(P_0+P_1)|(P_0+P_1)\Psi_a^{(+)}\rangle$$

over $b$, we obtain

$$\sigma_a=\frac{2\pi}{\hbar v_0}\sum_b\left|\left\langle\chi_b^{(-)}\right|Q\hat{H}(P_0+P_1)\right|$$
$$\times(P_0+P_1)\Psi_a^{(+)}\Big|^2\delta(E_a-E_b)$$
$$=-\frac{2}{\hbar v_0}\mathrm{Im}\langle\Psi_a^{(+)}(P_0+P_1)|V_{\mathrm{op}}^{P_0+P_1\to Q}|(P_0+P_1)\Psi_a^{(+)}\rangle. \quad \text{(A5)}$$

Here $\chi_b^{(-)}$ are states from the $Q$ subspace, and

$$(E_b-Q\hat{H}Q)|\chi_b^{(\pm)}\rangle=0, \quad \text{(A6)}$$

$$V_{\mathrm{op}}^{P_1+P_0\to Q}=(P_0+P_1)\hat{H}Q\frac{1}{E-Q\hat{H}Q+i\eta}Q\hat{H}(P_0+P_1)$$
$$\approx P_0\hat{H}Q\frac{1}{E-Q\hat{H}Q+i\eta}Q\hat{H}P_0$$
$$+P_1\hat{H}Q\frac{1}{E-Q\hat{H}Q+i\eta}Q\hat{H}P_1. \quad \text{(A7)}$$

We have discarded the terms

$$P_0\hat{H}Q\frac{1}{E-Q\hat{H}Q+i\eta}Q\hat{H}P_1$$

and

$$P_1\hat{H}Q\frac{1}{E-Q\hat{H}Q+i\eta}Q\hat{H}P_0.$$

This step corresponds to the so-called random-phase approximation, when the smallness of the discarded terms compared with those included is ensured by the mutual cancellation of the contributions of various channels.[135] In this approximation

$$\sigma_a\approx\sigma_a^{(1)}+\sigma_a^{(\infty)}\equiv\sigma_a^{(1)}+\Delta\sigma_a, \quad \text{(A8)}$$

where

$$\sigma_a^{(1)}=-\frac{2}{\hbar v_0}\mathrm{Im}\left\langle\Psi^{(+)}P_0\left|P_0\hat{H}Q\frac{1}{E-Q\hat{H}Q+i\eta}Q\hat{H}P_0\right|\right.$$
$$\left.\times P_0\Psi^{(+)}\right\rangle \quad \text{(A9)}$$

and

$$\sigma_a^{(\infty)}=-\frac{2}{\hbar v_0}\mathrm{Im}\left\langle\Psi^{(+)}P_1\left|P_1\hat{H}Q\frac{1}{E-Q\hat{H}Q+i\eta}Q\hat{H}P_1\right|\right.$$
$$\left.\times P_1\Psi^{(+)}\right\rangle. \quad \text{(A10)}$$

In the description of the target nucleus we restrict ourselves to the independent-particle model. We write $P_1=\Sigma_{n=1}^{\infty}P_{1n}$, where the operator $P_{1n}$ projects onto the subspace of nuclear excited states with $n$ particles and $n$ holes. Replacing $P_1$ by $P_{11}$ in (A10), we obtain the expression for the cross section for annihilation after a single inelastic collision:

$$\sigma_a^{(2)}=-\frac{2}{\hbar v_0}\mathrm{Im}\left\langle\Psi^{(+)}P_{11}\left|P_{11}\hat{H}Q\frac{1}{E-Q\hat{H}Q+i\eta}Q\hat{H}P_{11}\right|\right.$$
$$\left.\times P_{11}\Psi^{(+)}\right\rangle. \quad \text{(A11)}$$

We isolate the effective potential in (A1):

$$(P_0+P_1)V_{ef}(P_1+P_0)=(P_0+P_1)\left[\sum_{j=1}^{A}v_{\bar{p}j}+\hat{H}Q\right.$$

$$\times\frac{1}{E-Q\hat{H}Q+i\eta}Q\hat{H}\Bigg](P_0+P_1), \tag{A12}$$

where $v_{\bar{p}j}$ is the potential energy of the interaction between the antiproton and the $j$th nucleon of the nucleus.

The Lippmann–Schwinger equation can be obtained for the $t$ matrix describing the elastic scattering of an antiproton on the nucleus:

$$P_0TP_0=P_0UP_0+P_0UP_0G_0P_0TP_0, \tag{A13}$$

where the generalized optical potential is

$$U=V_{ef}+V_{ef}P_1GP_1V_{ef}, \tag{A14}$$

$$G^{-1}=G_0^{-1}-P_1V_{ef}P_1, \tag{A15}$$

$$G_0^{-1}=E-\hat{H}_N-\hat{H}_{\bar{p}}+i\eta. \tag{A16}$$

Here $H_N$ and $H_{\bar{p}}$ are the Hamiltonians of the target nucleus and a freely moving antiproton.

Substituting $V_{ef}$ from (A12) into (A14), we obtain the following approximate expression for $U$:

$$\begin{aligned}U\approx&\Bigg\{\sum_{j=1}^{A}v_{\bar{p}j}+\hat{H}Q\frac{1}{E-Q\hat{H}Q+i\eta}Q\hat{H}\Bigg\}+\sum_{j=1}^{A}v_{\bar{p}j}\\&\cdot P_1GP_1\cdot\sum_{j'=1}^{A}v_{\bar{p}j'}\\=&\Bigg\{\sum_{j=1}^{A}v_{\bar{p}j}+\sum_{j=1}^{A}v_{\bar{p}j}\cdot P_1GP_1\cdot\sum_{j'=1}^{A}v_{\bar{p}j'}\Bigg\}\\&+\hat{H}Q\frac{1}{E-Q\hat{H}Q+i\eta}Q\hat{H}\\=&U_{in}+U_a,\end{aligned} \tag{A17}$$

where

$$\begin{aligned}U_{in}=&\sum_{j=1}^{A}v_{\bar{p}j}\cdot P_1GP_1\cdot\sum_{j'=1}^{A}v_{\bar{p}j'}+\sum_{j=1}^{A}v_{\bar{p}j'}\\\approx&\sum_{j=1}^{A}\{v_{\bar{p}j}+v_{\bar{p}j}\cdot P_1GP_1\cdot v_{\bar{p}j}\}=\sum_{j=1}^{A}t_{\bar{p}j}\end{aligned} \tag{A18}$$

is the term in the generalized optical potential describing antiproton inelastic scattering and

$$U_a=\hat{H}Q\frac{1}{E-Q\hat{H}Q+i\eta}Q\hat{H} \tag{A19}$$

is the contribution to the optical potential from antiproton annihilation processes. Here $t_{j\bar{p}}$ is the $t$ matrix for antiproton scattering on the $j$th nucleon of the nucleus.

In obtaining (A17) we neglected the contributions to $P_0UP_0$ from virtual transitions $P_0\to Q\to P_1\to P_0$, and in (A18) we restricted ourselves to the incoherent approximation $j=j'$ and used the fact that

$$t_{\bar{p}j}=v_{\bar{p}j}+v_{\bar{p}j}P_1GP_1v_{\bar{p}j}. \tag{A20}$$

Obviously, $\psi_1$, the solution of the wave equation with the optical potential $P_0UP_0$, satisfies the equation

$$v_{\bar{p}j}\psi_1=t_{\bar{p}j}\tilde{\psi}_1, \tag{A21}$$

where $\tilde{\psi}_1$ is the solution of the wave equation with the optical potential $P_0U_aP_0$.

## APPENDIX 2

The intermediate stage of calculation of $\sigma_a^{(2)}$ in the convolution approximation involves calculation of the sum $\Sigma_f\rho_{fi}^*(\mathbf{r}')\rho_{fi}(\mathbf{r})$ over excited states $f$ of the nucleus, where

$$\begin{aligned}\rho_{fi}(\mathbf{r})=&\frac{1}{A}\sum_{j=1}^{A}\int d\mathbf{R}_1...d\mathbf{R}_A\Phi_f^*(\mathbf{R}_1,...\mathbf{R}_A)\\&\times\delta(\mathbf{r}-\mathbf{R}_j)\Phi_i(\mathbf{R}_1,...\mathbf{R}_A)\end{aligned} \tag{A22}$$

is the transition density of the nucleus.

Using the completeness property of the set of functions $\Phi_f$, we obtain

$$\begin{aligned}\sum_f\rho_{fi}^*(\mathbf{r}')\rho_{fi}(\mathbf{r})=&\frac{1}{A^2}\int d\mathbf{R}_1...d\mathbf{R}_A\sum_{jj'}\Phi_i^*(\mathbf{R}_1,...\mathbf{R}_A)\\&\times\delta(\mathbf{r}'-\mathbf{R}_{j'})\delta(\mathbf{r}-\mathbf{R}_j)\Phi_i(\mathbf{R}_1,...\mathbf{R}_A).\end{aligned} \tag{A23}$$

Taking into account only terms with $j'=j$ (the incoherent approximation), we simplify (A23):

$$\sum_f\rho_{fi}^*(\mathbf{r}')\rho_{fi}(\mathbf{r})\cong\frac{1}{A}\delta(\mathbf{r}-\mathbf{r}')\rho(\mathbf{r}). \tag{A24}$$

Here

$$\begin{aligned}\rho(\mathbf{r})=&\frac{1}{A}\int d\mathbf{R}_1...d\mathbf{R}_A\Phi_i^*(\mathbf{R}_1,...\mathbf{R}_A)\\&\times\sum_{j=1}^{A}\delta(\mathbf{r}-\mathbf{R}_j)\Phi_i(\mathbf{R}_1,...\mathbf{R}_A)\end{aligned} \tag{A25}$$

is the nuclear density in the ground state, $\int\rho(\mathbf{r})d\mathbf{r}=1$.

The cross section $\sigma_a^{(2)}$ contains $\Sigma_f|\psi_{2f}(\mathbf{r})|^2$, where the function $\psi_{2f}(\mathbf{r})$ is determined by Eq. (3.18), i.e.,

$$\begin{aligned}\sum_f|\psi_{2f}(\mathbf{r})|^2=&A^2\int\frac{d\mathbf{q}}{(2\pi)^3}\int\frac{d\mathbf{q}^{\mathrm{I}}}{(2\pi)^3}\tau^{\bar{N}N}(\mathbf{q})\tau^{\bar{N}N*}(\mathbf{q}^{\mathrm{I}})\\&\times\int d\mathbf{r}^{\mathrm{I}}...\int d\mathbf{r}^{\mathrm{IV}}G_{\mathrm{op}}^{(2)}\\&\times(\mathbf{r}|\mathbf{r}^{\mathrm{I}})G_{\mathrm{op}}^{(2)*}(\mathbf{r}|\mathbf{r}^{\mathrm{III}})\\&\times\sum_f\rho_{fi}(\mathbf{r}^{\mathrm{III}})\rho_{fi}^*(\mathbf{r}^{\mathrm{IV}})e^{-i\mathbf{q}(\mathbf{r}^{\mathrm{I}}-\mathbf{r}^{\mathrm{II}})}\\&\times e^{i\mathbf{q}^{\mathrm{I}}}(\mathbf{r}^{\mathrm{III}}-\mathbf{r}^{\mathrm{IV}})\tilde{\psi}_{1i}(\mathbf{r}^{\mathrm{I}})\tilde{\psi}_{1i}^*(\mathbf{r}^{\mathrm{III}}).\end{aligned} \tag{A26}$$

We substitute (A25) into (A26). Setting in the integral

$$\int\rho(\mathbf{r})e^{i(\mathbf{q}-\mathbf{q}')\mathbf{r}}d\mathbf{r},\quad\mathbf{q}\cong\mathbf{q}',$$

i.e.,

$$\int \rho(\mathbf{r})e^{i(\mathbf{q}-\mathbf{q}')\mathbf{r}}d\mathbf{r}\approx 1,$$

we obtain

$$\sum_f |\psi_{2f}(\mathbf{r})|^2 = A\int d\mathbf{r}^{\mathrm{II}}\int d\mathbf{r}^{\mathrm{I}} G_{\mathrm{op}}^{(2)}(\mathbf{r}|\mathbf{r}^{\mathrm{I}})G_{\mathrm{op}}^{(2)*}(\mathbf{r}|\mathbf{r}^{\mathrm{II}}) \times \int \frac{d\mathbf{q}}{(2\pi)^3}\int \frac{d\mathbf{q}^{\mathrm{I}}}{(2\pi)^3}\tau^{\bar{N}N}(\mathbf{q})\tau^{\bar{N}N*}(\mathbf{q}^{\mathrm{I}}) \times e^{-i\mathbf{q}\mathbf{r}^{\mathrm{I}}}e^{i\mathbf{q}^{\mathrm{I}}\mathbf{r}^{\mathrm{II}}}\tilde{\psi}_{1i}(\mathbf{r}^{\mathrm{I}})\tilde{\psi}_{1i}^{*}(\mathbf{r}^{\mathrm{II}}), \quad (A27)$$

where

$$\tau^{\bar{N}N}(\mathbf{q}) = \int d\mathbf{r}e^{i\mathbf{q}\mathbf{r}}t^{\bar{N}N}(\mathbf{r}). \quad (A28)$$


[1] B. O. Kerbikov, L. A. Kondratyuk, and M. G. Sapozhnikov, Usp. Fiz. Nauk **159**, 3 (1989) [Sov. Phys. Usp. **32**, 739 (1989)].
[2] O. D. Dal'karov and V. A. Karmanov, Fiz. Elem. Chastits At. Yadra **18**, 1399 (1987) [Sov. J. Part. Nucl. **18**, 599 (1987)].
[3] L. A. Kondratyuk and M. G. Sapozhnikov, in *Proc. of the Twentieth* LIYaF *Winter School on Nuclear Physics* (Leningrad Nuclear Physics Institute, Leningrad, 1985) [in Russian], p. 297.
[4] J. Cugnon and J. Vandermeulen, Ann. Phys. (Paris) **14**, 49 (1989).
[5] G. E. Walker, in *Relativistic Dynamics and Quark–Nuclear Physics*, edited by M. B. Johnson and A. Picklesimer (Wiley, New York, 1986), p. 267.
[6] M.-C. Lemaire, in *Medium Energy Nucleon and Antinucleon Scattering*, Lecture Notes in Physics, Vol. 243, edited by H. V. von Geramb (Springer, Berlin, 1985), p. 285; H. Heiselberg *et al.*, *ibid.*, p. 347; F. Myhrer, *ibid.*, p. 68; C. B. Dover, *ibid.*, p. 80.
[7] W. G. Love, A. Klein, and M. A. Franey, *Antinucleon– and Nucleon–Nucleus Interactions*, edited by G. E. Walker *et al.* (Plenum, New York, 1985), p. 1; C. B. Dover and D. J. Millener, *ibid.*, p. 25; D. Garreta, *ibid.*, p. 49.
[8] H. Heiselberg, A. S. Jensen, A. Miranda *et al.*, Phys. Scr. **40**, 141 (1989).
[9] Antiproton 1984, *Proc. of the Seventh European Symp. on Antiproton Interactions*, edited by M. R. Pennington (Adam Hilger, Ltd., Bristol, 1984); Antiproton 1986, *Proc. of the Eighth European Symp. on $\bar{N}N$ Interactions*, edited by S. Kharalambours *et al.* (World Scientific, Singapore, 1987).
[10] *Proc. of the Intern. Conf. on Nucleon–Antinucleon Interactions*, Moscow, ITEP, June 1991, Yad. Fiz. **55**, Nos. 5, 6 (1992) [Sov. J. Nucl. Phys. **55**, Nos. 5, 6 (1992)].
[11] M. L. Goldberger and K. M. Watson, *Collision Theory* (Wiley, New York, 1964) [Russian transl., Mir, Moscow, 1967, p. 707].
[12] A. K. Kerman, H. McManus, and R. M. Thaler, Ann. Phys. (N.Y.) **8**, 551 (1959).
[13] M. L. Goldberger and K. M. Watson, *Collision Theory* (Wiley, New York, 1964) [Russian transl., Mir, Moscow, 1967, p. 203].
[14] R. J. Glauber, in *Lectures in Theoretical Physics*, edited by W. E. Britten (Interscience, New York, 1959), Vol. 1, p. 315.
[15] A. G. Sitenko, Usp. Fiz. Nauk **67**, 377 (1959) [Soc. Phys. Usp. **2**, 195 (1959)].
[16] A. G. Sitenko, *The Theory of Nuclear Reactions* [in Russian] (Énergoatomizdat, Moscow, 1983).
[17] Yu. D. Prokoshkin, Fiz. Elem. Chastits At. Yadra **18**, 503 (1987) [Sov. J. Part. Nucl. **18**, 210 (1987)]; S. A. Bunyatov, Fiz. Elem. Chastits At. Yadra **10**, 657 (1979) [Sov. J. Part. Nucl. **10**, 259 (1979)].
[18] M. V. Hynes, *Relativistic Dynamics and Quark–Nuclear Physics*, edited by M. B. Johnson and A. Picklesimer (Wiley, New York, 1986), p. 499.
[19] R. Golub and H. Yoshiki, Nucl. Phys. **A501**, 869 (1989); H. Yoshiki and R. Golub, Nucl. Phys. **A536**, 648 (1992).
[20] G. I. Budker and A. N. Skrinskiĭ, Usp. Fiz. Nauk **124**, 561 (1978) [Sov. Phys. Usp. **21**, 277 (1978)].
[21] F. E. Mills, in *Proc. of the Symp. Antimatter 87*, Karlsruhe, 1987, Hyperfine Interaction **44**, 31 (1988); D. C. Peaslee, *ibid.*, p. 37; H. Koch, *ibid.*, p. 59; C. D. Johnson and T. R. Sherwood, *ibid.*, p. 65.
[22] P. Stankus, Nucl. Phys. **A544**, 603c (1992).
[23] W. W. Buck *et al.*, Phys. Rev. C **33**, 234 (1986).
[24] V. F. Andreev *et al.*, Yad. Fiz. **51**, 142 (1990) [Sov. J. Nucl. Phys. **51**, 88 (1990)]; V. F. Andreev *et al.*, Nuovo Cimento A **103**, 1163 (1989).
[25] V. P. Zavarzina and A. V. Stepanov, Izv. Akad. Nauk SSSR, Ser. Fiz. **55**, 960 (1991) [Bull. Acad. Sci. USSR, Phys. Ser.].
[26] V. P. Zavarzina and A. V. Stepanov, Yad. Fiz. **54**, 44 (1991) [Sov. J. Nucl. Phys. **54**, 27 (1991)].
[27] V. P. Zavarzina and A. V. Stepanov, Yad. Fiz. **43**, 854 (1986) [Sov. J. Nucl. Phys. **43**, 543 (1986)].
[28] J. Rafelski, Phys. Lett. **91B**, 281 (1980); **207B**, 371 (1988); S. C. Phatak and N. Sarma, Phys. Rev. C **36**, 864 (1987).
[29] J. Formanek, Czech. J. Phys. B **31**, 1256 (1981); V. Simak, Czech. J. Phys. B **31**, 1341 (1981); D. Strottman and W. R. Gibbs, Phys. Lett. **149B**, 288 (1984); E. M. Friedlander and M. Plumer, Phys. Rev. C **40**, 2410 (1989); J. Cugnon, Nucl. Phys. **A542**, 559 (1992).
[30] F. Balestra *et al.*, Phys. Scr. **44**, 323 (1991).
[31] F. Balestra *et al.*, *Antiproton 1984, Proc. of the Seventh European Symp. on Antiproton Interactions*, edited by M. R. Pennington (Adam Hilger, Ltd., Bristol, 1984), p. 251; Czech. J. Phys. B **36**, 340 (1986); G. Piragino, in *Hadronic Physics at Intermediate Energy*, edited by T. Bressani and R. A. Ricci (North-Holland, Amsterdam, 1986), p. 293; Yu. A. Batusov, S. A. Bunjatov, I. V. Falomkin *et al.*, Europhys. Lett. **2**, 115 (1986).
[32] V. P. Zavarzina and A. V. Stepanov, Izv. Russ. Akad. Nauk, Ser. Fiz. **56**, 153 (1992) [Bull. Russ. Acad. Sci., Phys. Ser.].
[33] V. P. Zavarzina and A. V. Stepanov, Yad. Fiz. **56**, 206 (1993) [Phys. At. Nucl. **56**, 260 (1993)].
[34] D. Agassi and D. S. Koltun, Ann. Phys. (N.Y.) **140**, 1 (1982); H. Feshbach, A. Kerman, and S. Koonin, Ann. Phys. (N.Y.) **125**, 429 (1980); A. J. Koning and J. M. Akkermans, Ann. Phys. (N.Y.) **208**, 216 (1991).
[35] H. C. Chiang and J. Hüfner, Nucl. Phys. **A349**, 466 (1980); W. Q. Chao, F. Hachenberg, and J. Hüfner, Nucl. Phys. **A384**, 24 (1982).
[36] K. Masutani and K. Yazaki, Phys. Lett. **104B**, 1 (1981); Nucl. Phys. **A407**, 309 (1983).
[37] D. Garreta, P. Birien, G. Bruge *et al.*, Phys. Lett. **135B**, 266 (1984).
[38] D. Garreta, P. Birien, G. Bruge *et al.*, Phys. Lett. **149B**, 64 (1984); **151B**, 473 (1985).
[39] R. C. Barrett and D. F. Jackson, *Nuclear Sizes and Structure* (Clarendon Press, Oxford, 1977) [Russian transl., Naukova Dumka, Kiev, 1981].
[40] H. Heiselberg, A. S. Jensen, A. Miranda *et al.*, Nucl. Phys. **A446**, 637 (1985).
[41] K.-I. Kubo, H. Toki, and M. Igarashi, Nucl. Phys. **A435**, 708 (1985).
[42] K.-I. Kubo, F. Iseki, and H. Toki, Phys. Lett. **153B**, 195 (1985).
[43] Y. Oki, K. Tamuro, and Y. Sakamoto, Nuovo Cimento A **103**, 397 (1990).
[44] C. I. Batty, E. Friedman, and I. Lichtenstadt, Phys. Lett. **142B**, 241 (1984); Nucl. Phys. **A436**, 621 (1985).
[45] E. Friedman and I. Lichtenstadt, Nucl. Phys. **A455**, 573 (1986).
[46] L. A. Kondratyuk, M. Zh. Shmatikov, and R. Bidzarri, Yad. Fiz. **33**, 795 (1981) [Sov. J. Nucl. Phys. **33**, 413 (1981)].
[47] L. A. Kondratyuk and M. Zh. Shmatikov, Yad. Fiz. **38**, 361 (1983) [Sov. J. Nucl. Phys. **38**, 216 (1983)].
[48] O. D. Dal'karov and V. A. Karmanov, Pis'ma Zh. Eksp. Teor. Fiz. **39**, 288 (1984) [JETP Lett. **39**, 345 (1984)]; Phys. Lett. **147B**, 1 (1984); Pis'ma Zh. Eksp. Teor. Fiz. **41**, 47 (1985) [JETP Lett. **41**, 58 (1985)].
[49] O. D. Dalkarov and V. A. Karmanov, Nucl. Phys. **A445**, 579 (1985); Zh. Eksp. Teor. Fiz. **89**, 1122 (1985) [Sov. Phys. JETP **62**, 645 (1985)].
[50] L. A. Kondratyuk and M. G. Sapozhnikov, Yad. Fiz. **46**, 89 (1987) [Sov. J. Nucl. Phys. **46**, 56 (1987)].
[51] V. A. Sergeev and V. P. Zavarzina, Czech. J. Phys. B **36**, 347 (1986).
[52] V. P. Zavarzina and V. A. Sergeev, Preprint P-0505, Nuclear Research Institute, USSR Academy of Sciences, Moscow (1986) [in Russian]; Yad. Fiz. **46**, 486 (1987) [Sov. J. Nucl. Phys. **46**, 261 (1987)].
[53] V. M. Kolybasov and L. A. Kondratyuk, Yad. Fiz. **18**, 316 (1973) [Sov. J. Nucl. Phys. **18**, 162 (1973)]; Phys. Lett. **39B**, 439 (1972).
[54] G. Faldt and A. Ingemarsson, J. Phys. G **9**, 261 (1983).
[55] V. P. Zavarzina, V. A. Sergeev, and A. V. Stepanov, Yad. Fiz. **49**, 1316 (1989) [Sov. J. Nucl. Phys. **49**, 818 (1989)].
[56] I. I. Levintov, Dokl. Akad. Nauk SSSR **107**, 240 (1956) [Sov. Phys. Dokl. **1**, 175 (1957)]; G. Faisner, *Nucleon Polarization in Scattering* [in Russian] (IIL, Moscow, 1960).
[57] R. Birsa, F. Bradamante, S. Dalla Torre-Colautti *et al.*, Phys. Lett.

**155B**, 437 (1985); A. Martin, R. Birsa, K. Bos *et al.*, Nucl. Phys. **A487**, 563 (1988).
[58] J. Mahalanabis, Z. Phys. A **326**, 131 (1987).
[59] Tan-Zhen-Qiang and Gu Yunting, Chinese J. Nucl. Phys. **12**, 201 (1990).
[60] W.-H. Ma and D. Strottman, Phys. Rev. C **44**, 615 (1991).
[61] Tan-Zhen-Qiang and Ma Wei-Hsing, Nuovo Cimento A **103**, 185 (1990).
[62] J. W. Wilson and L. W. Townsend, Can. J. Phys. **59**, 1569 (1981); J. W. Wilson, Phys. Lett. **52B**, 149 (1974); W. G. Love, *Microscopic Optical Potentials*, edited by H. V. von Geramb (Springer, New York, 1979), p. 350; D. M. Brink, *ibid.*, p. 340.
[63] R. M. De Vries and J. C. Peng, Phys. Rev. C **22**, 1055 (1980); Phys. Rev. Lett. **43**, 1373 (1979).
[64] V. A. Sergeev, Kratk. Soobshch. Fiz. No. 8, 44 (1989) [in Russian].
[65] S. Kox *et al.*, Phys. Lett. **159B**, 15 (1985); Phys. Rev. C **35**, 1678 (1987); Nucl. Phys. **A420**, 162 (1984).
[66] N. J. Di Giacomo and R. M. De Vries, Commun. Nucl. Part. Phys. A **12**, 111 (1984).
[67] V. P. Zavarzina and A. A. Stepanov, Yad. Fiz. **49**, 113 (1989) [Sov. J. Nucl. Phys. **49**, 71 (1989)].
[68] V. P. Zavarzina and A. A. Stepanov, Fiz. Elem. Chastits At. Yadra **19**, 932 (1988) [Sov. J. Part. Nucl. **19**, 404 (1988)].
[69] V. P. Zavarzina and A. A. Stepanov, Kratk. Soobshch. Fiz. No. 3, 7 (1991) [in Russian].
[70] J. D. Walecka, Ann. Phys. (N.Y.) **83**, 491 (1974).
[71] W. M. Gibson and B. R. Pollard, *Symmetry Principles in Elementary Particle Physics* (Cambridge University Press, Cambridge, 1976) [Russian transl., Atomizdat, Moscow, 1979].
[72] A. Bouyssy and S. Marcos, Phys. Lett. **114B**, 397 (1982).
[73] B. C. Clark, S. Hama, J. A. McNeil *et al.*, Phys. Rev. Lett. **53**, 1423 (1984).
[74] B. C. Clark, in *Medium Energy Nucleon and Antinucleon Scattering*, edited by H. V. von Geramb (Springer, New York, 1985), p. 391.
[75] R. Bonetti and M. S. Hussein, J. Phys. G **12**, L119 (1986).
[76] C. B. Dover and J. M. Richard, Phys. Rev. C **21**, 1466 (1980).
[77] R. A. Bryan and R. J. N. Phillips, Nucl. Phys. **B5**, 201 (1968).
[78] J. Cote *et al.*, Phys. Rev. Lett. **48**, 1319 (1982).
[79] P. H. Timmers, W. A. van der Sanden, and J. J. De Swart, Phys. Rev. D **29**, 1928 (1984); **30**, 1995 (1984).
[80] R. Vinh Mau, in *Medium Energy Nucleon and Antinucleon Scattering*, edited by H. V. von Geramb (Springer, New York, 1985), p. 3.
[81] W. G. Love, A. Klein, M. A. Franey *et al.*, *ibid.*, p. 160.
[82] A. Picklesimer, P. C. Tandy, and J. A. Tjon, Phys. Lett. **163B**, 311 (1985).
[83] T. Jaroszewicz and S. J. Brodsky, Phys. Rev. C **43**, 1946 (1991).
[84] M. Thies, Nucl. Phys. **A478**, 571c (1988).
[85] T. Suzuki and M. Narumi, Phys. Lett. **125B**, 251 (1983).
[86] T. Suzuki and M. Narumi, Nucl. Phys. **A426**, 413 (1984).
[87] J. Kronenfeld, A. Gal, and J. M. Eisenberg, Nucl. Phys. **A430**, 525 (1984).
[88] T. Suzuki, Nucl. Phys. **A444**, 659 (1985).
[89] S. Adachi and H. V. von Geramb, in *Medium Energy Nucleon and Antinucleon Scattering*, edited by H. V. von Geramb (Springer, New York, 1985), p. 310.
[90] H. V. von Geramb, K. Nakano, and L. Rikus, Lett. Nuovo Cimento **42**, 209 (1985).
[91] S. Adachi and H. V. von Geramb, Nucl. Phys. **A470**, 461 (1987).
[92] J. Mahalanabis and H. V. von Geramb, Nucl. Phys. **A493**, 412 (1989).
[93] D. Murdock and C. J. Horowitz, in *Antinucleon- and Nucleon–Nucleus Interactions*, edited by G. E. Walker *et al.* (Plenum, New York, 1985), p. 135.
[94] C. J. Horowitz and D. Murdock, in *Medium Energy Nucleon and Antinucleon Scattering*, edited by H. V. von Geramb (Springer, New York, 1985), p. 437.
[95] C. J. Horowitz and D. Murdock, Phys. Rev. C **37**, 2032 (1988); **35**, 1442 (1987).
[96] M. L. Goldberger, Phys. Rev. **74**, 1269 (1948).
[97] E. Clementel and C. Villi, Nuovo Cimento **11**, 176 (1955).
[98] L. Verlet and J. Gavoret, Nuovo Cimento **10**, 505 (1958).
[99] A. S. Davydov, *Nuclear Theory* [in Russian] (Fizmatgiz, Moscow, 1958).
[100] K. Kikuchi and M. Kawai, *Nuclear Matter and Nuclear Reactions* (North-Holland, Amsterdam, 1968).
[101] M. P. Duerr, Phys. Rev. **109**, 1347 (1958).
[102] V. P. Zavarzina, V. A. Sergeev, and A. V. Stepanov, in *Proc. of the Symp. on Nucleon–Nucleon and Hadron–Nucleus Interactions at Intermediate Energies* [in Russian] (Leningrad Nuclear Physics Institute Press, Leningrad, 1986), p. 565; Kratk. Soobshch. Fiz. No. 6, 6 (1986) [in Russian].
[103] D. K. Harrington and G. K. Varma, Nucl. Phys. **A306**, 477 (1978).
[104] M. L. Goldberger and K. M. Watson, *Collision Theory* (Wiley, New York, 1964) [Russian transl., Mir, Moscow, 1967, p. 703].
[105] I. E. McCarthy and D. L. Pursey, Phys. Rev. **122**, 578 (1961).
[106] R. T. Janus and I. E. McCarthy, Phys. Rev. C **10**, 1041 (1974).
[107] N. S. Zelenskaya and I. B. Teplov, Fiz. Elem. Chastits At. Yadra **11**, 342 (1979) [Sov. J. Part. Nucl. **11**, 126 (1980)].
[108] N. S. Zelenskaya and I. B. Teplov, *Exchange Processes in Nuclear Reactions* [in Russian] (Moscow State University Press, Moscow, 1985), p. 125.
[109] K. Amos and F. D. Marzio, Z. Phys. A **322**, 137 (1985); Phys. Rev. C **29**, 1914 (1984); **31**, 561 (1984).
[110] H. Iwasaki *et al.*, Nucl. Phys. **A433**, 580 (1985).
[111] M. R. Clover, R. M. De Vries, N. J. Di Giacomo *et al.*, Phys. Rev. C **26**, 2138 (1982).
[112] A. S. Il'inov, V. L. Matushko, and S. E. Chigrinov, Yad. Fiz. **36**, 878 (1982) [Sov. J. Nucl. Phys. **36**, 513 (1982)].
[113] A. S. Iljinov, V. I. Nazaruk, and S. E. Chigrinov, Nucl. Phys. **A382**, 378 (1982).
[114] M. Cahay, J. Cugnon, and J. Vandermeulen, Nucl. Phys. **A393**, 237 (1983).
[115] J. Cugnon and J. Vandermeulen, Phys. Rev. C **36**, 2726 (1987).
[116] A. S. Botvina, Y. S. Golubeva, and A. S. Iljinov, Preprint 742/91, Nuclear Research Institute, Moscow (1991).
[117] Y. S. Golubeva, A. S. Iljinov, A. S. Botvina *et al.*, Nucl. Phys. **A483**, 539 (1988).
[118] Y. S. Golubeva, A. S. Iljinov, B. V. Krippa *et al.*, Nucl. Phys. **A537**, 393 (1992).
[119] F. Uchiyama, Prog. Theor. Phys. **82**, 869 (1989).
[120] J. Cugnon and J. Vandermeulen, Phys. Lett **146B**, 16 (1984).
[121] J. Cugnon and J. Vandermeulen, Phys. Rev. C **39**, 181 (1989).
[122] V. I. Nazaruk, Yad. Fiz. **46**, 80 (1987) [Sov. J. Nucl. Phys. **46**, 51 (1987)]; Kratk. Soobshch. Fiz. No. 2, 46 (1989) [in Russian]; Phys. Lett. **155B**, 323 (1985).
[123] V. M. Kolybasov and Yu. N. Sokol'skikh, Pis'ma Zh. Eksp. Teor. Fiz. **51**, 434 (1990) [JETP Lett. **51**, 489 (1990)]; V. M. Kolybasov *et al.*, Phys. Lett. **222B**, 135 (1989).
[124] A. E. Kudryavtsev and V. E. Tarasov, Yad. Fiz. **54**, 59 (1991) [Sov. J. Nucl. Phys. **54**, 36 (1991)].
[125] E. Hernandez and E. Oset, Nucl. Phys. **A455**, 584 (1986).
[126] E. Hernandez and E. Oset, Phys. Lett. **184B**, 1 (1987).
[127] E. Hernandez and E. Oset, Nucl. Phys. **A493**, 453 (1989).
[128] G. E. Brown, C. B. Dover, P. B. Siegel *et al.*, Phys. Rev. Lett. **60**, 2723 (1988); G. E. Brown and M. Rho, Phys. Lett. **237B**, 3 (1990).
[129] G. E. Brown and M. Rho, Phys. Rev. Lett. **66**, 2720 (1991).
[130] G. E. Brown, A. Sethi, and N. M. Hintz, Phys. Rev. C **44**, 2653 (1991).
[131] A. Hosaka and H. Toki, Nucl. Phys. **A529**, 429 (1991).
[132] J. Cugnon and J. Vandermeulen, Phys. Lett **279B**, 5 (1992).
[133] V. Mull, K. Holinde, and J. Speth, Phys. Lett. **275B**, 12 (1992).
[134] H. W. Barz, G. Bertsch, P. Danielewicz *et al.*, Phys. Lett. **275B**, 19 (1992).
[135] V. V. Balashov, *Quantum Collision Theory* [in Russian] (Moscow State University Press, Moscow, 1985), p. 121.

Translated by Patricia A. Millard